

Pricing American Options with Monte Carlo Methods



Kellogg College
University of Oxford

A thesis submitted for the degree of
MSc in Mathematical Finance
Trinity 2018

Contents

1	Introduction and Overview	2
1.1	Numerical methods for option pricing	2
1.1.1	Finite differences	2
1.1.2	Lattice-based methods	3
1.1.3	Monte Carlo	3
1.2	Main findings and outline	3
2	Risk Neutral Pricing	5
2.1	European options	6
2.2	American options	6
3	Monte Carlo methods	8
3.1	Simulating random paths	8
3.2	European options	9
3.3	American options	10
3.4	The Longstaff-Schwartz Algorithm for American Options	12
4	Effects of respecting no-arbitrage bounds	16
4.1	American call on a single asset	21
4.2	American put on a single asset without dividends	22
4.3	American Max Call	29
4.4	American Exchange Option	41
5	Conclusions and Outlook	47
	Bibliography	47
A	Data	52

List of Figures

3.1	Algorithm for pricing a European option	9
3.2	Generic algorithm for a Monte Carlo pricer	11
3.3	Longstaff-Schwartz algorithm	14
3.4	Exercise region for American max call	15
4.1	Modified Longstaff-Schwartz algorithm respecting no-arbitrage bounds . .	17
4.2	Ensemble of Monte Carlo paths for an out-of-the-money American put . . .	19
4.3	Exercise boundary for the American put	25
4.4	Overview over the modification of the exercise behaviour for the American put	26
4.5	Prices for the American put	27
4.6	Change of basis functions for the American put	28
4.7	Change of interpolation order for the American put	29
4.8	Prices for the American max call on non-dividend paying assets	32
4.9	Exercise boundary for the American max call on non-dividend paying assets	34
4.10	Overview over the exercise behaviour for the American max call on non-dividend paying assets	35
4.11	Overview over the modification of the exercise behaviour for the American max call on non-dividend paying assets	36
4.12	Prices for the American max call on dividend paying assets	37
4.13	Overview over the modification of the exercise behaviour for the American max call	38
4.14	Change of basis functions for the American max call	39
4.15	Change of interpolation order for the American max call	40
4.16	Overview over the modification of the exercise behaviour for the American exchange option	43
4.17	Prices for the American exchange option	44
4.18	Change of basis functions for the American max call	45
4.19	Change of interpolation order for the American exchange option	46

List of Tables

4.1	Overview over the lower and upper bounds derived in the following subsections.	18
4.2	Parameter of the American put	24
4.3	Computational speed for the American put option	24
4.4	Parameters for the American max call on non-dividend paying underlying assets	31
4.5	Computational speed for the American max call without dividends	31
4.6	Parameters for the American max call on dividend paying underlying assets	33
4.7	Computational speed for the American max call with dividends	35
4.8	Parameters for the American exchange option	42
4.9	Computational speed for the American exchange option	42
A.1	Prices for the American put	53
A.2	Prices for the American max call	54
A.3	Prices for the American exchange option	55

Abstract

Pricing American options on multiple underlying assets is a challenging, high-dimensional problem that is frequently tackled using the Longstaff-Schwartz method [1], regressing the continuation value over all Monte Carlo paths in order to decide on early exercise. We extend this approach by requiring the interpolated continuation value to satisfy no-arbitrage constraints. We apply this extension to the pricing problem of an American put on a single underlying asset, an American max call on two underlying assets, and an American exchange option, while also varying the number and type of basis functions of the interpolation of the continuation value. We demonstrate that respecting no-arbitrage bounds has a noticeable impact on the calculated price of the option, especially when there are only few Monte Carlo paths sampling the in-the-money region of the payoff at expiry.

Chapter 1

Introduction and Overview

American options are common instruments in today's markets. While pricing them using finite differences works well for options on assets with few degrees of freedom (a single underlying or a basket with few components), underlying assets with high dimensionality (ie baskets with many components) typically require using different numerical approaches. In the following subsections, we first give a short overview over the various numerical approaches to option pricing, and conclude with the main contributions of this thesis.

1.1 Numerical methods for option pricing

1.1.1 Finite differences

The most straight-forward way to solve the equations governing the time-evolution of the price of an option is to approximate derivatives using finite differences, an approach pioneered by Schwartz [2]. In these methods, the operator $\frac{\partial}{\partial S}$ is approximated using the central approximation, and the second derivative $\frac{\partial^2}{\partial t^2}$ using the standard approximation. The time derivative $\frac{\partial}{\partial t}$ can be approximated in different ways, leading to three separate methods: The explicit method uses the backwards approximation. The implicit method use the forwards approximation. The Crank Nicholson method uses a central approximation and is numerically stable [3]. Rannacher time-stepping [4, 5] that replaces the first few Crank Nicholson steps with implicit Euler (half-) time-steps can be employed to recover second order convergence.

The early exercise right of American options leads to a free boundary condition. Various approaches have been devised to address this, eg front fixing via Landau transformation [6, 7] or solving the linear complementarity problem via policy iteration [8, 9, 10, 11].

Approximating the partial differential equation governing the time evolution of the option price using finite differences is most practical when dealing with a low-dimensional problem, eg options on single or few underlying assets.

1.1.2 Lattice-based methods

Lattice-based methods model the future prices of the underlying asset on the nodes of a binomial (or multinomial) tree. Cox, Ross, and Rubinstein [12] introduced a pricer for European and American options on a single underlying using a binomial tree. The tree's nodes carry the underlying asset's prices, and its edges carry the transition probabilities, generally taken to be risk-neutral, although other measures have been employed as well, see eg [13, 14]. Brennan and Schwartz [15] and Rubinstein [16] showed the equivalence of lattice and explicit finite difference methods. Boyle [17] and Kamrad and Richkin [18] extended lattice based methods to cover options with more than one state variables.

Although lattice-based methods are well-suited for introducing the concept of risk-neutral measures from a pedagogical point of view and allow for a straight-forward implementation of the early exercise rights of American options, their main draw-back is the fact that their run-time complexity is exponential in the number of nodes.

1.1.3 Monte Carlo

Boyle [19] first suggested using Monte Carlo method to approximate the price of an option, already pointing out control variates [20] to improve the $\propto (n_{\text{path}})^{-\frac{1}{2}}$ scaling¹ of the standard deviation of the Monte Carlo simulation. Other variance reduction techniques include the use of antithetic variables and importance sampling, see eg Chapter 4 of [21] for an introduction. Quasi Monte Carlo methods using low discrepancy sequences [22, 23] are an alternative approach to accelerating convergence, although they reformulate the pricing problem as a proper integral.

It is straightforward and computationally rather efficient to incorporate additional degrees of freedom in Monte Carlo pricers [19] for European options.

For American options, the straightforward extension of performing nested Monte Carlo simulations for the option price for each path at each time step is computationally prohibitively expensive. Various regression methods have been devised [1, 24, 25, 26], giving lower bounds for the price of the option due to the fact that the error introduced via the regression will result in a suboptimal exercise strategy. Rogers' algorithm [27, 28] provides an upper bound for the option price using a dual formulation of the pricing problem.

1.2 Main findings and outline

We investigate modifications of the Longstaff-Schwartz [1] method for pricing American options based on no-arbitrage bounds of the continuation value. As in its original approach, the continuation value is approximated by regressing over all Monte Carlo paths. It has

¹ n_{path} is the number of Monte Carlo paths.

been noted before that interpolation effects can lead to negative continuation values, see eg Example 8.6.1 in [21].

We note that interpolation effects can also cause other undesirable behaviour: in regions of the space of underlying asset prices which are in-the-money, but only relatively poorly sampled by Monte-Carlo paths, the interpolated continuation might violate no-arbitrage constraints, see Figures 4.2 and 4.3 for an example in the case of an American put on a single underlying asset. We suggest extending the Longstaff-Schwartz method by enforcing no-arbitrage constraints on the continuation value. Of course, this has to be done on a case-by-case basis for a given option type, so it is not a modification that only needs to be implemented once. One has to analytically derive no-arbitrage bounds for each given option type.

Deriving these constraints for the American put in Section 4.2, the American max call in Section 4.3, and the American exchange option in Section 4.4, we analyse the impact on the resulting price from Monte Carlo simulations, using an interpolation of order 2 for the continuation value with monomials, Chebyshev polynomials, and Hermite polynomials.

It turns out respecting no-arbitrage bounds can have quite a large effect on the price – changing it by up to 10% when applied to an American max call on non-dividend paying assets where the no-arbitrage bounds actually exclude early exercise, see Figure 4.12. We see that changing the interpolation order or the function basis used in the interpolation of the continuation value to Chebyshev or Hermite polynomials impacts the computed price as well, see eg Figures 4.14 and 4.15. The magnitude of the effect of respecting no-arbitrage bounds depends on the option under investigation. In our examples, it ranges from not statically significant (for the American put on a single asset) over 0.5% (for the American max call on dividend paying assets) and 3% (for the American exchange option) to 10% for the American max call on non-dividend paying assets.

In order to check our numerical Python implementation of the no-arbitrage Ansatz, we tested the code against the toy example of [1] and various other option prices we found in the literature.

Chapter 2 gives a brief review of risk neutral pricing to settle the notation. Chapter 3 discusses Monte Carlo methods for option pricing. Chapter 4 presents the main results of this thesis. Chapter 5 contains the conclusion and outlook to possible further work.

Chapter 2

Risk Neutral Pricing

Introductions to the mathematics of financial derivatives can be found in various textbooks [29, 30, 31, 32, 33]. This section gives a brief overview over risk neutral pricing to settle the notation.

Consider a model economy consisting of n_S risky assets S_i and a risk-free asset β . The risk-free asset β obeys the differential equation

$$d\beta(t) = \beta(t)r(t)dt, \quad (2.1)$$

with $r(t)$ is the (possibly random/time varying) risk free interest rate.

In the real world measure \mathbb{P} , the assets S_i obey the following stochastic differential equation

$$dS_i(t) = S_i(t)(\mu_i(t)dt + \sigma_i(t)dW_i^{\mathbb{P}}), \quad (2.2)$$

where $\mu_i(t)$ is the asset-dependent drift term, $\sigma_i(t)$ the asset's volatility, and $dW^{\mathbb{P}}$ an n_S -dimensional standard Brownian motion.

In a complete market, it can be shown that the price $V(S(t_0), t_0)$ of a European style contract – ie where the option can only be exercised at maturity – at time $t_0 < t_1$ is given by the expected value of the future price $V(S(t_1), t_1)$ with respect to the risk neutral measure \mathbb{Q}

$$V(S(t_0), t_0) = \mathbf{E}^{\mathbb{Q}} \left[V(S(t_1), t_1) \frac{\beta(t_0)}{\beta(t_1)} \right], \quad (2.3)$$

see eg Equation (5.2.31) in [33] or Theorem 12.3.2 in [34] for a formal treatment. The measure \mathbb{Q} is unique if the market is arbitrage-free.

Risk neutral in this context refers to the fact that in this measure, all the drift terms of

the risky assets S_i are given by the risk free interest rate r :

$$dS_i(t) = S_i(t) \left[r(t)dt + \sigma_i dW_i^{\mathbb{Q}}(t) \right], \quad (2.4)$$

where σ_i is the asset's volatility and $W_i^{\mathbb{Q}}(t)$ is a standard Brownian motion in the \mathbb{Q} measure. It can be shown that $W_i^{\mathbb{Q}}(t)$ is related to $W_i^{\mathbb{P}}(t)$ via

$$dW_i^{\mathbb{Q}}(t) = dW_i^{\mathbb{P}}(t) + \nu(t)_i dt, \quad (2.5)$$

where $\nu_i(t)$ satisfies $\mu(t) = r(t) + \sigma_i \nu_i(t)$ (no summation over i). Note that the volatilities σ_i remain unchanged under this change of measure, so that it is possible to estimate σ_i from real world observations of the assets' S_i price processes.

Combining (2.1) and (2.4) immediately shows that S_i/β is a drift-free process

$$d\left(\frac{S_i}{\beta(t)}\right) = \left(\frac{S_i}{\beta(t)}\right) \sigma_i dW_i^{\mathbb{Q}}, \quad (2.6)$$

and hence (2.3) holds.

2.1 European options

In particular, setting t_1 to maturity T in (2.3), the price of a European option at time t is given by

$$V(S(t), t) = \mathbf{E}^{\mathbb{Q}} \left[h(S(T), T) \exp \left(- \int_t^T r(s) ds \right) \right], \quad (2.7)$$

where $h(S, T)$ is the payoff of the option at maturity, eg

$$h(S, T) = \begin{cases} \max[S - K, 0], & \text{for a call option,} \\ \max[K - S, 0], & \text{for a put option,} \end{cases} \quad (2.8)$$

with K the strike of the option. This translates into a computer algorithm rather easily, see Figure 3.1.

2.2 American options

In contrast to European options, the holder of an American option may exercise at any point in time up to and including maturity. From this qualitative difference – ie that the option holder has more rights in the American case as opposed to the European case – it is clear that the price of an American option must be at least as high as the price of a corresponding European option.

During the lifetime of an American option, the option holder must continuously monitor the price of the underlying asset and decide whether the price of the option is larger than the instantaneous payoff they would receive if they exercised the option at this moment in time. It can be shown that the price $V(S, t)$ of an American option is given by

$$\boxed{V(S(t), t) = \sup_{\tau \in [t, T]} \mathbf{E}^{\mathbb{Q}} \left[\exp \left(- \int_t^{\tau} r(s) ds \right) h(S(\tau)) \right]}, \quad (2.9)$$

where the supremum is obtained for the optimal stopping time τ^*

$$\tau^* = \inf_{t \geq 0} \left\{ V(S(t), t) \leq h(S(t)) \right\}, \quad (2.10)$$

which is the first instance in time at which the price of the option is smaller than the payoff the option holder would receive if they exercised at this point in time, see eg Equations (8.2) and (8.3) in [21].

Chapter 3

Monte Carlo methods

Using Monte Carlo methods to price structured products is well established, see eg [21]. In particular for multidimensional problems, eg derivatives with multiple underlying assets, these methods provide an efficient approximation of the price of an option. This is especially true for European style options, but American options can be priced relatively efficiently as well.

The basic idea behind this approach for an option with payoff h is the following. Creating a (large enough) sample of paths of random processes of the form (2.4) for the underlying stochastic processes, the price of the derivative is obtained by explicitly computing the expected value of the discounted payoff (2.7) using these paths.

3.1 Simulating random paths

In order to simulate the paths of the underlying assets, we need to solve the following system of coupled stochastic differential equations

$$dS_i(t) = S_i(t) \left(r(t)dt + \sigma_i dW_i^{\mathbb{Q}}(t) \right), \quad (3.1)$$

where \vec{W} is an n -dimensional \mathbb{Q} -Brownian motion with correlation matrix ρ_{ij} , and $r(t)$ is the deterministic interest rate.

This is most conveniently done using the Euler-Maruyama scheme. A detailed introduction can be found in [21]. In summary, simulating random paths on a time mesh $t_j = t_0 + jdt$, $j = 1 \dots n_{\text{step}}$, step size dt , amounts to computing

$$S_i(t + dt) = S_i(t) \left(1 + r(t)dt + \sqrt{dt} \sum_j B_{ij} Z_j(t) \right), \quad (3.2)$$

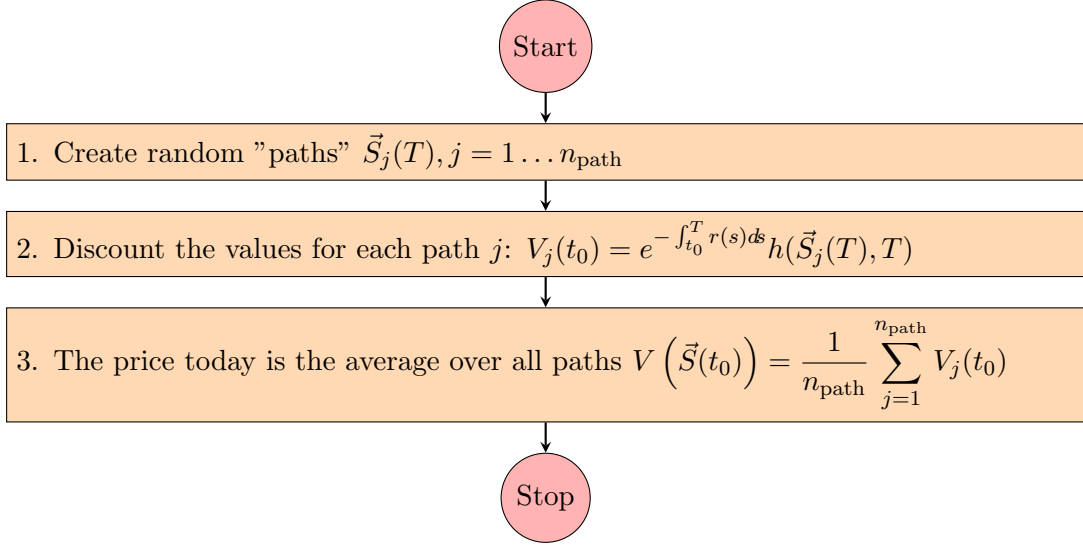


Figure 3.1: The algorithm for pricing a European option is a straight-forward implementation of (2.7). Simulate path number j for underlying i that starts at today's value of the underlying $\vec{S}_j(0) = S_i(0)$ by taking a single step to maturity $\vec{S}_j(T)$. Discount the value of the payoff for each path to today to obtain V_j . The price of the option today is then given by the average over the V_j , with its error estimated by the standard deviation of the V_j .

for each time step dt or in matrix form

$$\vec{S}(t + dt) = \vec{S}(t) \left(\vec{1} + r(t)dt\vec{1} + \sqrt{dt}\mathbf{B} \cdot \vec{Z} \right), \quad (3.3)$$

where the multiplication is component-wise and $Z_j(t)$ are uncorrelated random numbers. \mathbf{B} is a matrix that factorizes the covariance matrix $\Sigma = \mathbf{B}\mathbf{B}^T$ and can be obtained via Cholesky decomposition. The covariance matrix $\Sigma_{ij} = \rho_{ij}\sigma_i\sigma_j$ encodes the correlation ρ_{ij} and variances σ_i of the assets (no sum over i, j).

3.2 European options

For a European option, only the end-point of the paths is relevant for the payoff and can be sampled exactly in the Black-Scholes model without Euler-Maruyama time-stepping. After creating an ensemble of random values for the value of the underlying assets at maturity $S_i^j(T)$, we can compute the value of the payoff at maturity for each path. Taking the average of the discounted payoffs of each simulated path gives the price of the option today, see Figure 3.1. The uncertainty in the price can be estimated using the standard deviation.

3.3 American options

For an American option however, the situation is somewhat more complex. At each time step, the option holder has to make a (rational) choice – to exercise the option at the current time step or to hold on to the option. In fact, if the price of the American option (that would be obtained by holding onto the option) is smaller than the payoff, the option holder should exercise immediately, see (2.10).

Figure 3.2 describes a generic algorithm for pricing an American option on n_{asset} underlying assets using a Monte Carlo approach. The basic idea is that after creating the random paths, the algorithm goes backwards in time: First, create the ensemble of random paths $\vec{S}_j(t_i)$ with path labels $j = 1 \dots n_{\text{path}}$ and discrete time step $t_i, i = 0 \dots T$ of length dt . Perform the following steps for each path: At maturity, set the value of the option to the payoff $V_j(T) = h(\vec{S}_j(T))$. Now iterate backwards in time by first discounting the price along each path and compute the continuation value – ie the value of the option that the holder would achieve if they held on to the option in the current time step. Compare the former with the latter and decide for each path whether or not to exercise. Modify the price at this time step accordingly. Iterate these steps until the first time step. As it makes no sense to have the option holder exercise the option in the moment of buying it, compute the price of the option along each path for the initial time t_0 by simple discounting from the first time step t_1 to t_0 without comparing it to the continuation value.

The price of the option at t_0 is then simply given by the average over all n_{path} paths.

In principle, computing the continuation value $c = v(\vec{S}_j(t_i), t_i)$ in step 6 of Figure 3.2 requires a full revaluation of the option price at each time step with a new set of random paths. This strategy scales with the square of the number of paths, making it prohibitively expensive to compute. Hence, various strategies have been proposed to reduce this computational complexity [1, 24, 25, 26].

In general, these strategies produce sub-optimal stopping times (2.10) so that the resulting price of the option is a lower bound (2.9). Other approaches result in upper bounds for the option price by solving a dual problem [27, 35].

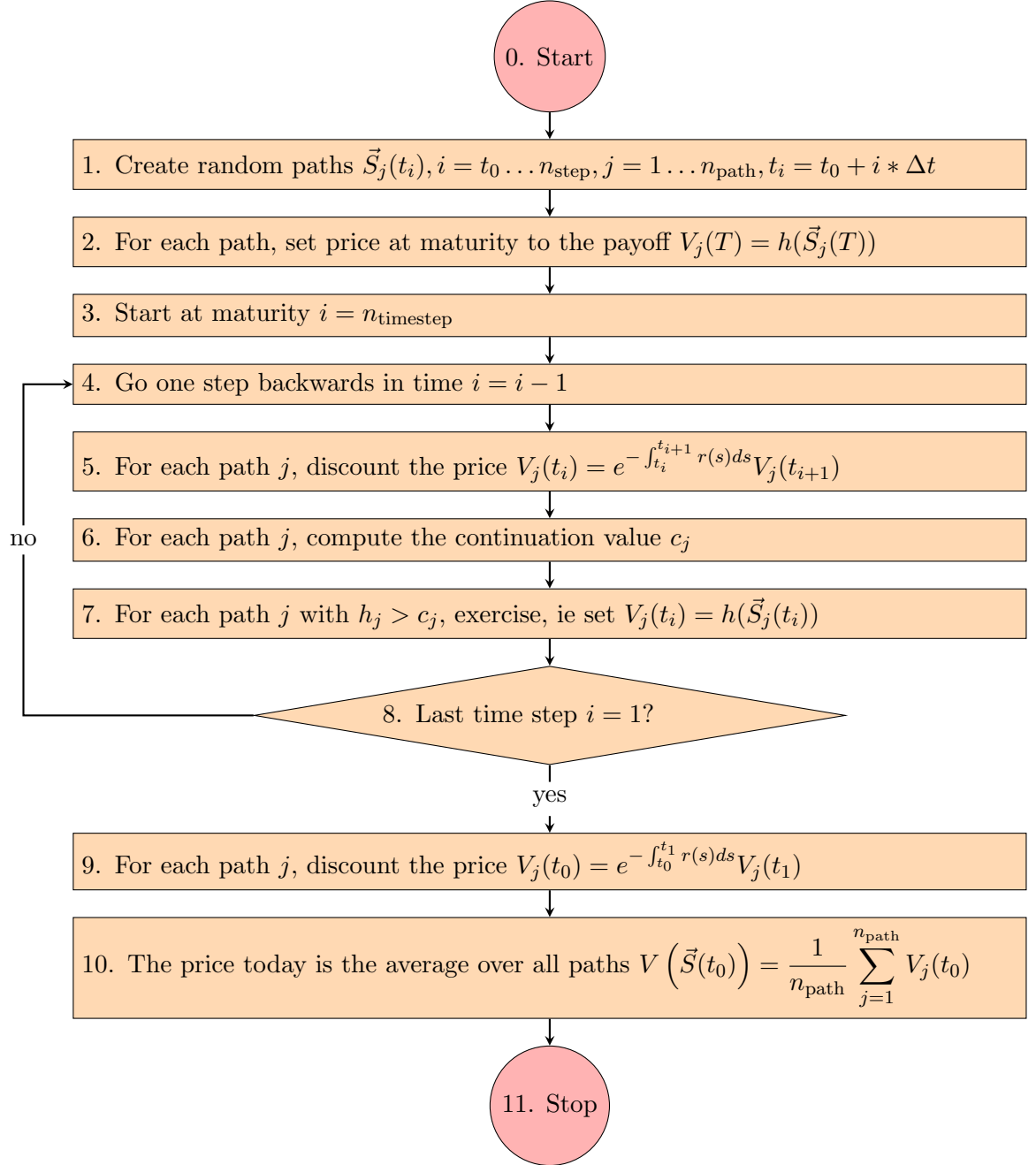


Figure 3.2: A generic algorithm for computing the price of an American option using a Monte Carlo strategy using continuation values to decide whether or not to exercise early.

3.4 The Longstaff-Schwartz Algorithm for American Options

[1, 24, 25, 26] use regression methods to compute the continuation value in step 6 of Figure 3.2. We will focus on the Longstaff-Schwartz method [1] and mention differences to [24, 25, 26] only in passing.

As mentioned previously, computing the continuation value of an option is computationally rather expensive. [1] suggest approximating the continuation value at each time step using a least squares regression over all n_{path} paths, see steps 6a and 6b in Figure 3.3.

At each time step t_i , expand the continuation value $c(\vec{S})$ (as a function of the underlying asset price) in terms of a function basis ψ_j .

$$c(\vec{x}, t_i) = \mathbf{E} \left[V(\vec{S}(t_{i+1})) \middle| \vec{S}(t_i) = \vec{x} \right] = \sum_{k=0}^{n_{\text{order}}} \beta_k \psi_k(\vec{x}). \quad (3.4)$$

where the expansion coefficients β_k are obtained by a least squares fit to the (discounted) values of the option at the next time step:

$$\beta = (B_{\psi\psi})^{-1} B_{V\psi}, \quad (3.5)$$

where $B_{\psi\psi}, B_{V\psi}$ at time step t_i are given by

$$(B_{v\psi})_{\ell} = \mathbf{E} \left[V(\vec{S}(t_{i+1})) \psi_{\ell}(\vec{S}(t_i)) \right], \quad (3.6)$$

$$(B_{\psi\psi})_{k\ell} = \mathbf{E} \left[\psi_k(\vec{S}(t_i)) \psi_{\ell}(\vec{S}(t_i)) \right], \quad (3.7)$$

and the expectation is over the ensemble of paths¹.

Using this least squares regression for the continuation value results in the algorithm in Figure 3.3. [39] proved almost sure convergence of this algorithm in the limit of infinitely many sample paths.

In contrast to simulating the early exercise decision by setting the price

$$V_j(t_i) = h(\vec{S}_j(t_i)), \quad (3.8)$$

for all paths j where $h(\vec{S}_j(t_i)) > e^{-\int_{t_i}^{t_{i+1}} r(s)ds} V_j(t_{i+1})$ in step 7, [26] assume that the non-exercised value is the continuation value

$$V_j(t_i) = \max \left[c(\vec{S}_j(t_i)), h(\vec{S}_j(t_i)) \right], \quad (3.9)$$

which has the drawback of accumulating the sampling error from the difference between c

¹For numerical stability, it is advisable to not invert the matrix $B_{\psi\psi}$ in (3.5) but instead use a least squares solver to solve $B_{\psi\psi}\beta = B_{V\psi}$ directly for β . We use `numpy.linalg.lstsq` from the Python [36] packages NumPy [37] and SciPy [38].

and V . Hence we keep using (3.8) instead.

Deciding on early exercise by comparing $c(\vec{S}(t_i), t_i)$ to the immediate payoff $h(\vec{S}(t_i), t_i)$ typically results in a sub-optimal exercise pattern. Hence, by virtue of (2.10), the resulting price of the option today is a lower bound on the option's true price.

This approach is trading the complexity of running a full Monte Carlo valuation for each path at each time step for a least squares fit to a set of basis functions with $n_{asset} \times n_{order}$ terms. The order of expansion n_{order} and the set of basis functions ψ_j should be tuned to each option under investigation, incorporating any prior knowledge about the option at hand.

Employing the Longstaff-Schwartz algorithm as described above, the continuation value can violate no-arbitrage bounds. For example, [21] noted in example 8.6.1 that the continuation value of an American max call can become negative through interpolation effects: in the blue region in the (S_0, S_1) space of Figure 3.4, a naive application of the Longstaff-Schwartz algorithm leads to early exercise as the continuation value is negative and hence smaller than the payoff (which is bounded by 0 from below).

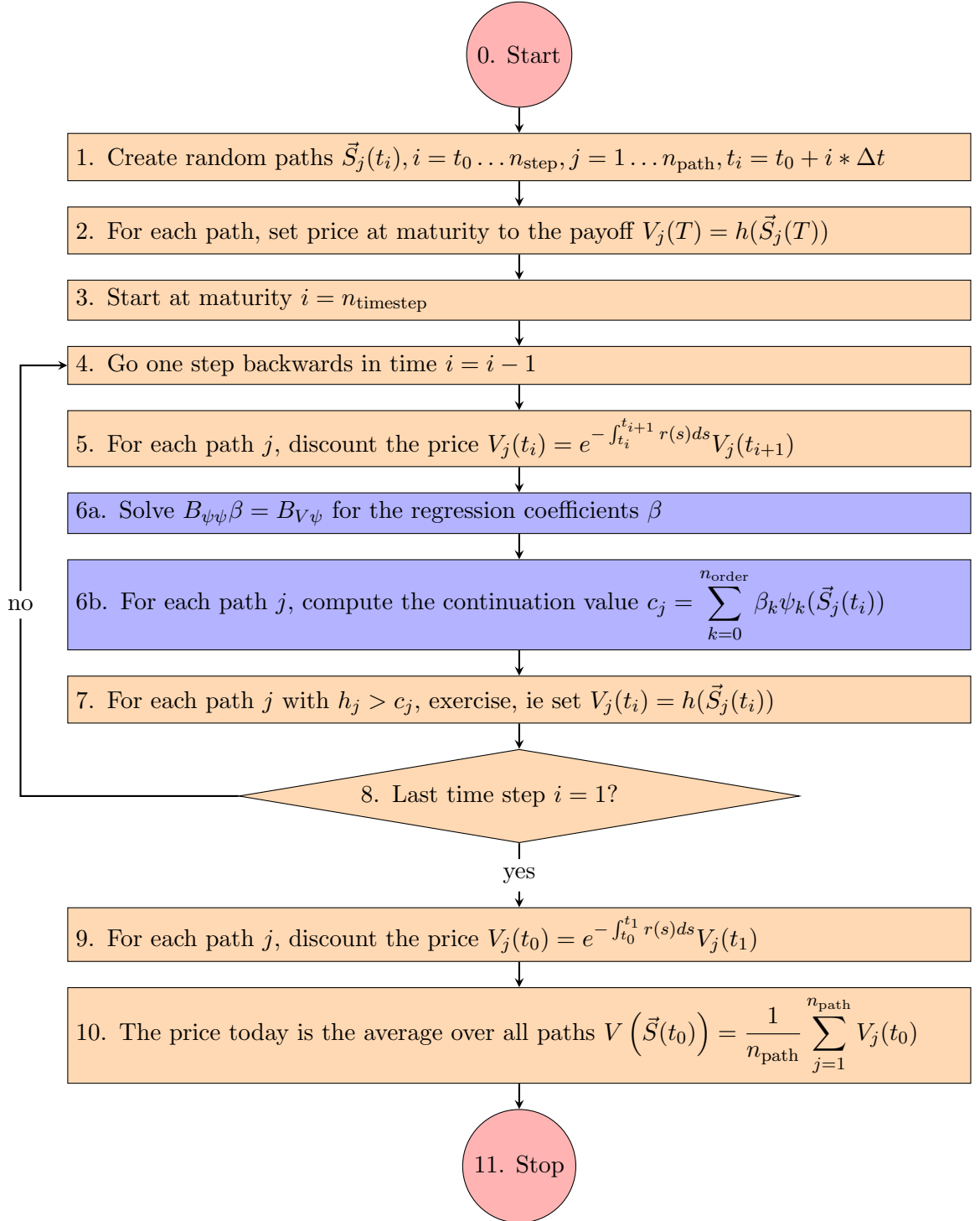


Figure 3.3: The generic pricing algorithm from Figure 3.2, detailing the Longstaff-Schwartz approach to computing the continuation value c via least squares regression in step 6. Steps 6a and 6b in the purple boxes detail the solution of Equation (3.5) to obtain (3.4).

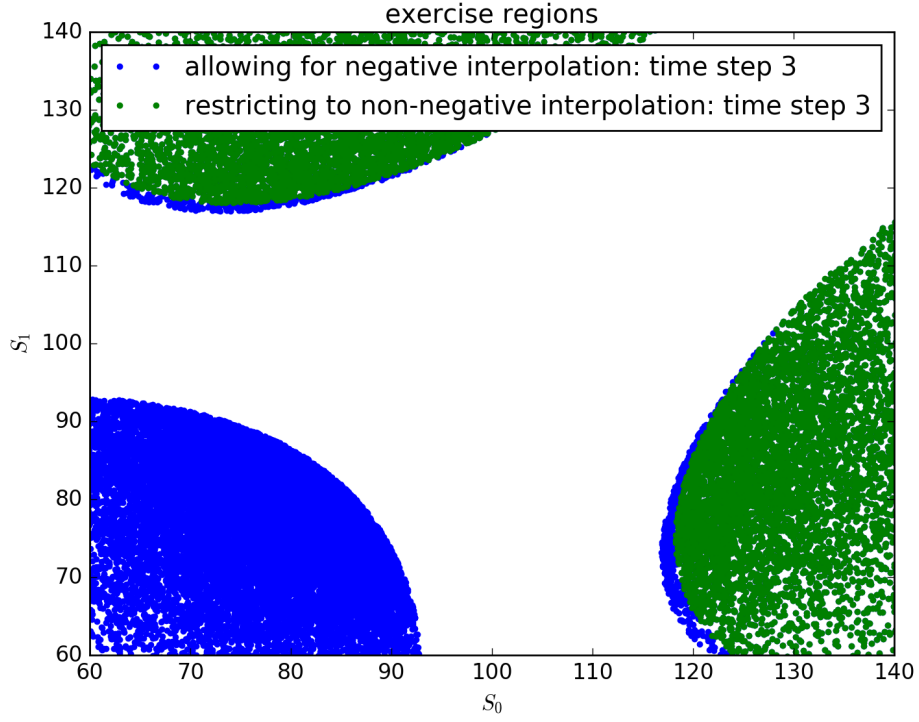


Figure 3.4: Plot of the exercise regions for an American max call on two assets with payoff $P = (\max(S_0, S_1) - K)^+$ and the following parameters: initial values $S_0(0) = S_1(0) = 100$, volatilities $\sigma_0 = \sigma_1 = 0.2$, dividend yields $y_0 = y_1 = 0.1$, strike $K = 100$, interest rate $r = 0.05$, maturity $T = 3$, and 9 exercise opportunities (see Example 8.6.1 and Figure 8.9 in [21]). Differences in the Figure are caused by differing choices of basis functions for the interpolation). The Longstaff-Schwartz least squares interpolation of the expected value for both runs used all terms up to and including order 2: $(1, S_0, S_1, S_0^2, S_1^2, S_0 S_1)$. Bounding the continuation value by 0 from below (green dots) removes the spurious early-exercise region for small values of S_0, S_1 (blue dots).

Chapter 4

Effects of respecting no-arbitrage bounds

Besides being non-negative (as mentioned in the previous chapter), prices of American options obey various other no-arbitrage constraints, eg an American put option is always more expensive than the corresponding European put, giving a lower bound on the continuation value.

The basic idea of this chapter can be summarized as follows. Bounding the continuation value from above b_u and below b_l by no-arbitrage arguments, we analyse the resulting changes in the prices for various American options.

The upper and lower bounds are enforced when computing the continuation value. At each time step t_i for each set of paths \vec{S} we compare

$$c_j = \max \left[\min \left[c_j^{\text{LS}}, b_u \right], b_l \right] \stackrel{?}{>} h \left(\vec{S}(t_i) \right), \quad (4.1)$$

where c_j^{LS} is the continuation value obtained via the Longstaff-Schwartz algorithm (3.4) at time step j , h is the payoff, \vec{S} is the vector of underlying assets, $b_{u,l}$ is the upper (lower) bound on the option price, and c_j is the new continuation value respecting no-arbitrage arguments. Enforcing the upper and lower bounds ensures arbitrage-freeness with minimal effort¹. Hence, inserting step 6c into the pricing algorithm in Figure 4.1 is all that is needed.

In general, computing the upper and lower bounds comes at the price of increased computational effort, so these modifications should in practice only be used if they lead to a noticeable change in option price.

¹By definition, the discounted values along each path do respect no-arbitrage bounds. Hence, the alternative to (4.1) of excluding points from the regression that violate no-arbitrage bounds is not viable. We did not explore other alternative strategies where eg one could attempt to integrate the no-arbitrage constraints in the set of basis functions such that the continuation value becomes a smooth function.

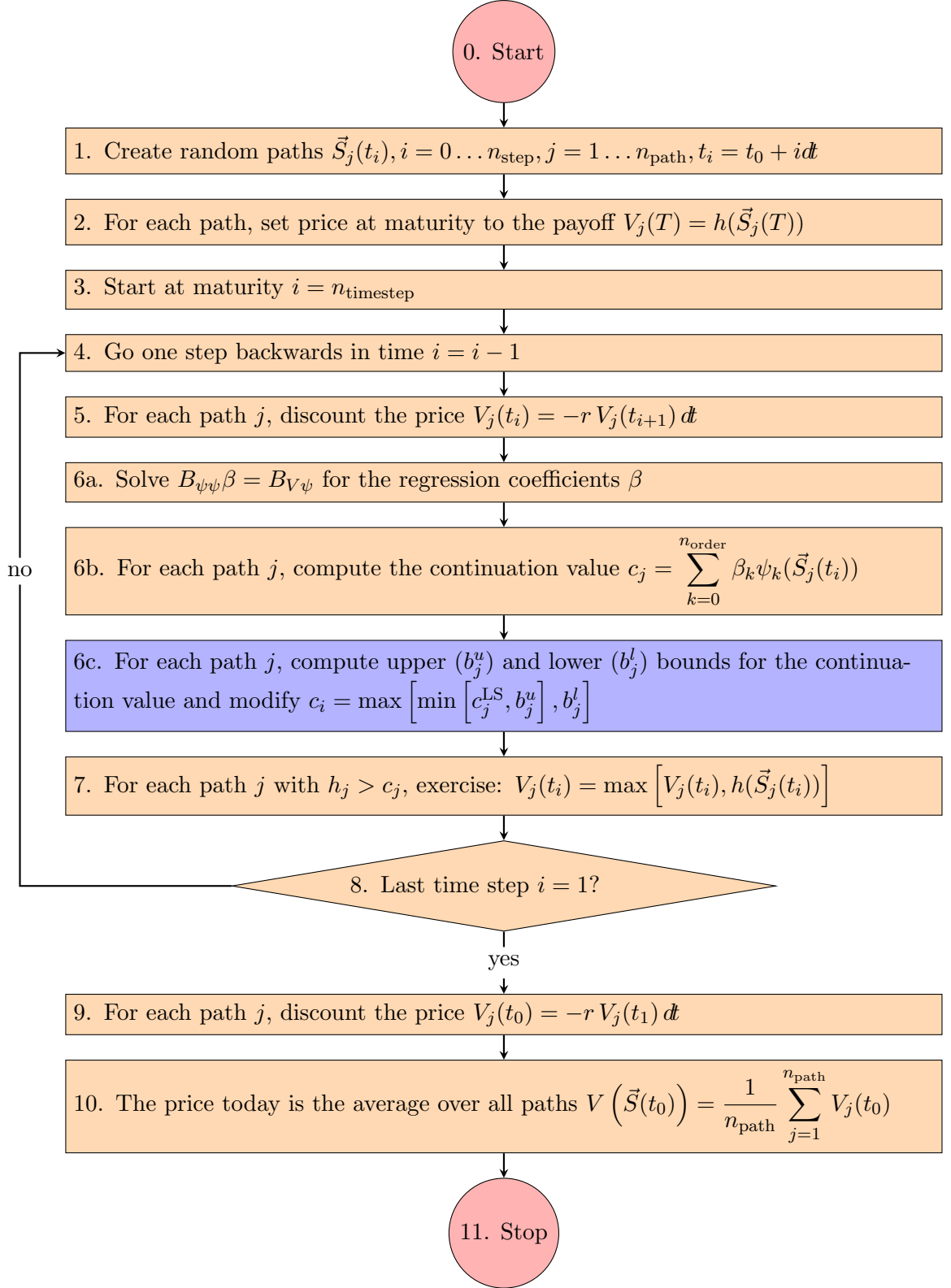


Figure 4.1: Respecting no-arbitrage bounds introduces the additional step 6c (purple box) into the pricing algorithm Figure 3.3. Ensuring that the continuation value respects no-arbitrage bounds compensates for the fact that for options that are out-of-the money, only a small subset of Monte Carlo paths probes the in-the-money region of the payoff.

Sub-section	Option type	payoff h	Lower bound	Upper bound
4.1	American call on a single asset without dividends	$\max[S - K, 0]$	C_e	
4.2	American put on a single asset	$\max[K - S, 0]$	$C_e + Ke^{-rT} - S$	$C_e + K - S$
4.3	American max call	$\max[\max_i[S_i], 0]$	$\max_i[C_e^{\text{ind}}(S_i)]$	$\sum_i S_i$
4.4	American exchange option	$\max[S_0 - S_1, 0]$	E_e	S_0

Table 4.1: Overview over the lower and upper bounds derived in the following subsections.

Lower and upper bounds

In each of the following sections, we derive lower and upper bounds for the price of the option under consideration, see Table 4.1 for a summary. In principle, it is also possible to employ numerical bounds (eg by employing finite difference schemes to approximate the value of a European option). Here, we focus on analytical bounds.

Results of the modification of Longstaff-Schwartz

In general, respecting lower and upper bounds has the largest impact on the option price when the option is deep out-of-the money, as in this case, the Monte Carlo paths only rarely come close to the strike. Let us focus on a single Monte Carlo path that is "lucky" enough to get close to the strike, see Figure 4.2. The continuation value for this path will likely be rather "wrong", as there are few paths that are probing deeper in-the-money regions and hence the least-squares regression will be biased by the out-of-the-money paths. Hence, interpolation effects may cause the continuation value to violate no-arbitrage bounds.

Effects of changing the function basis

Instead of using monomials as function basis in the underlying asset prices $S_i^{n_i}$, $i = 0 \dots n_{\text{asset}}, n = 0 \dots n_{\text{order}}$, various other choices of orthogonal polynomials are possible. For each option type, we investigate the effect of using Chebyshev and Hermite polynomials as function basis.

Hermite polynomials $H_n(x)$ can be defined either using the "probabilist" convention

$$H_n(x) = (-1)^n e^{\frac{x^2}{2}} \frac{d^n}{dx^n} e^{-\frac{x^2}{2}}, \quad (4.2)$$

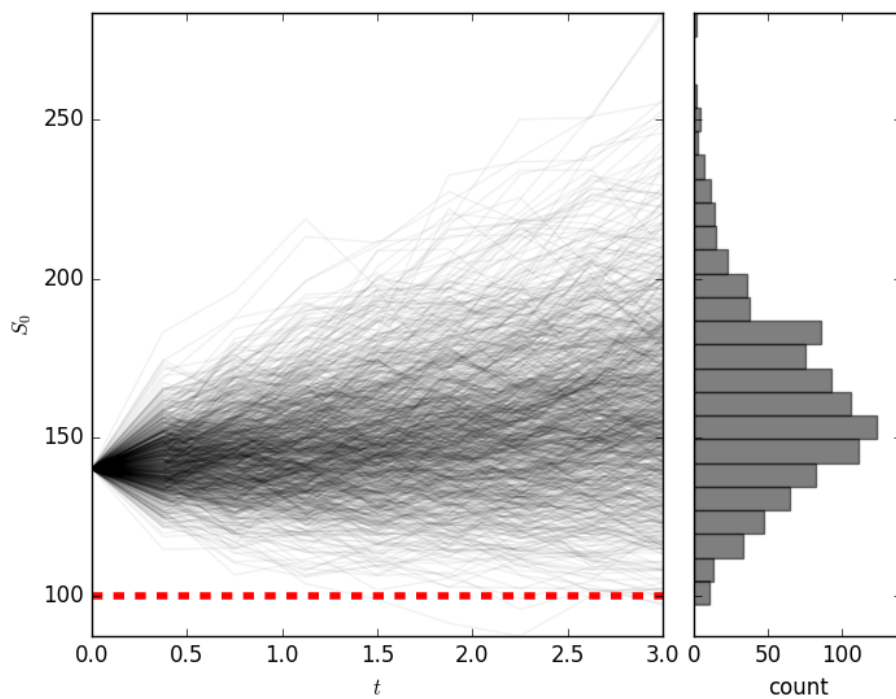


Figure 4.2: The Monte Carlo paths for an out-of-the-money American put only rarely approach the strike. The faint black lines are the simulated Monte Carlo paths. The dashed red line is the strike. The histogram on the right shows the distribution of the Monte Carlo paths at expiry. The continuation value of the bottom-most path is likely "wrong", as there is no set of paths surrounding it that is probing the in-the money region.

or the "physicist" convention

$$H_n(x) = (-1)^n e^{x^2} \frac{d^n}{dx^n} e^{-x^2}. \quad (4.3)$$

We use the latter convention as basis for the least squares interpolation.

Chebyshev polynomials of the first kind $T_n(x)$ are defined by the recursion relation

$$T_0 = 1, \quad (4.4)$$

$$T_1(x) = x, \quad (4.5)$$

$$T_n(x) = 2xT_{n-1}(x) - T_{n-2}(x). \quad (4.6)$$

It is known that they provide the best approximation to a continuous function under the maximum norm when using the Chebyshev nodes (ie their roots) for interpolation. However, as we do not have control over the position of the interpolation nodes, we do not observe a clear advantage of using them over Hermite polynomials or monomials.

We use (pseudo-)Vandermonde matrices to for the least squares interpolation². The Vandermonde matrix of order 3 for Hermite polynomials for a single underlying asset S_0 looks like

$$M = \begin{pmatrix} 1 & H_1((S_0)_1) & H_2((S_0)_1) & H_3((S_0)_1) \\ \vdots & \vdots & \vdots & \vdots \\ 1 & H_1((S_0)_{n_{\text{path}}}) & H_2((S_0)_{n_{\text{path}}}) & H_3((S_0)_{n_{\text{path}}}) \end{pmatrix}, \quad (4.7)$$

while the pseudo-Vandermonde matrix for Chebyshev polynomials of order 2 for two underlying assets S_0, S_1 has the form

$$M = \begin{pmatrix} 1 & T_1((S_0)_1) & T_1((S_1)_1) & T_2((S_0)_1) & T_2((S_1)_1) & T_1((S_0)_1)T_1((S_1)_1) \\ \vdots & \vdots & \vdots & \vdots & \vdots & \vdots \\ 1 & T_1((S_0)_{n_{\text{path}}}) & T_1((S_1)_{n_{\text{path}}}) & T_2((S_0)_{n_{\text{path}}}) & T_2((S_1)_{n_{\text{path}}}) & T_1((S_0)_{n_{\text{path}}})T_1((S_1)_{n_{\text{path}}}) \end{pmatrix}. \quad (4.8)$$

Here, $(S_i)_j$ is referring to the i -th component of vector \vec{S}_j where $j = 1 \dots n_{\text{path}}$ is the path number.

In addition to varying the basis functions themselves, we also analyse the effects of going from an order 2 to an order 3 expansion.

²See Section 2.8.1 of [40] for an introduction to Vandermonde matrices. Numpy [37] provides an efficient implementation of Vandermonde matrices for both Chebyshev, Hermite, and various other types of polynomials.

4.1 American call on a single asset

Asset without dividends

The following argument shows that the price of an American call on a non-dividend paying asset is exactly the same as the price of the corresponding European call. Let π be a portfolio consisting of an American call with payoff $(S - K)^+$ with price C_a and a single bond with nominal amount K and current value $Ke^{-r(T-t)}$. The value of this portfolio is obviously³

$$\pi(t) = C_a + Ke^{-r\tau} . \quad (4.9)$$

Now we need to analyse the hypothetical performance of the portfolio in dependence of the asset price⁴.

1. If the asset price is below the strike $S < K$ for all $t \leq T$, the option will be worthless, and the portfolio will be worth

$$\pi(T) = K . \quad (4.10)$$

2. If the asset price is below the strike for all $t < T$ and above the strike at maturity, it makes sense to hold on to the call until maturity, with the value of the portfolio

$$\pi(T) = \max[S(T) - K, 0] + K = \max[S(T), K] . \quad (4.11)$$

3. If at the asset price is above the strike at some point in time $t < T$, $S(t) > K$, exercising the call would yield

$$\pi(t) = S(t) - K + Ke^{-r(T-t)} < S(t) , \quad (4.12)$$

in other words, something that is worth less than the asset.

Exercising at maturity (if at all) will yield at least the asset, whereas exercising early yields less than the asset. In other words, holding on to the portfolio of the stock and the bond obtained through early exercise will leave the owner poorer than holding on to the call and possibly exercising at maturity.

As it is always optimal to exercise an American call on a non-dividend paying asset at maturity (if at all), the price of an American call must be the same as the price of a

³ S is the price of the underlying asset, K is the strike, τ is the time to maturity, r is the risk-free interest rate, and $(x)^+ \equiv \max(x, 0)$.

⁴Obviously, we cannot predict the future.

European call

$$\boxed{C_a = C_e} . \quad (4.13)$$

As this is a closed form solution for the American call, there is no need to price this via a Monte Carlo approach. However, this expression will be useful when deriving bounds on the continuation value of other options below.

4.2 American put on a single asset without dividends

Unlike the call option described in Section 4.1, the price of an American put is generally larger than the price of the corresponding European put.

In order to arrive at a lower and upper bound for the price of a simple American put, we make use of the put-call inequality for American options.

Put-call inequality for American options

While for European options, it is possible to derive what is known as put-call parity

$$\text{put} - \text{call} = \text{forward} , \quad (4.14)$$

using eg no arbitrage arguments, there is no such equality for American style options. Instead, an upper and a lower bound for the difference between the price of a simple American call and a put with strike K on the same underlying S with payoffs

$$h_{\text{call,put}} = \max [\pm (S - K) , 0] \quad (4.15)$$

can be derived for an American call C_a and put P_a on a single asset without dividends. The upper bound follows immediately from the fact that the price of an American put is larger than the price of a European put

$$P_a \geq P_e \stackrel{\text{put-call parity}}{=} C_e - S + Ke^{-rT} = C_a - S + Ke^{-rT} . \quad (4.16)$$

The lower bound can be derived by analysing the corresponding portfolio of one long American call, one short American put, one stock short and K in cash

$$\pi = C_a - P_a - S + K . \quad (4.17)$$

If the holder of the put decides to exercise early, the owner of the portfolio pays $\max(K-S, 0)$ and receives a stock in return, so that the portfolio's value is given by

$$\pi = \underbrace{C_a}_{\geq 0} - \underbrace{P_a}_{=K-S} - S + K \geq 0. \quad (4.18)$$

If the put is not exercised early, the portfolio's value at maturity is 0:

$$\pi = \begin{cases} \underbrace{C_a}_{=0} - \underbrace{P_a}_{=K-S} - S + K = 0, & \text{if } S < K, \text{ the put is exercised, the call is not exercised} \\ \underbrace{C_a}_{=S-K} - \underbrace{P_a}_{=0} - S + K = 0, & \text{if } S > K, \text{ the put is not exercised, the call is exercised} \\ \underbrace{C_a}_{=0} - \underbrace{P_a}_{=0} - S + K = 0, & \text{if } S = K \end{cases} \quad (4.19)$$

Hence this the value of the portfolio is larger than 0 at all times and so

$$C_a - P_a \geq S - K. \quad (4.20)$$

Putting upper and lower bound together, we find the put-call inequality for American options on non-dividend paying assets

$$S - K \leq C_a - P_a \leq S - Ke^{-rT}. \quad (4.21)$$

Lower and upper bounds

Making use of the fact that the price of an American call option on a single asset without dividends is the same as the price of a European call, $C_a = C_e$, (see Section 4.1), we immediately see from (4.21)

$$\boxed{C_e + K - S \geq P_a \geq C_e + Ke^{-rT} - S.} \quad (4.22)$$

Results of the modifications of Longstaff-Schwartz

Integrating the bounds (4.22) into the algorithm Figure 4.1⁵, the effect on the price of the option is statistically insignificant, independent of whether the option is in-the-money, at-the-money, or out-of-the money at inception, see Table A.1 and Figure 4.5. Table 4.2 describes the option's and valuation parameters.

Based on the arguments presented in Section 4, we would have expected to see a significant effect – if any at all – for out-of-the money options. Figure 4.3 shows that, when

⁵We use the Black-Scholes formula for computing the prices of the European calls.

parameter type	parameter	symbol	value
option	initial asset value	S_0	varying
	maturity	T	3
	strike	K	100
	risk-free interest rate	r	0.05
	volatility	σ	0.02
valuation	number of paths	n_{path}	10000
	number of time steps	n_{timestep}	9
	number of repetitions	n_{rep}	100
	Longstaff-Schwartz interpolation order		1, S , S^2

Table 4.2: Parameters of the American put. Each valuation was performed n_{rep} times, leading to the error bars quoted in Table A.1.

continuation value	no constraints	non-negative	respecting no-arbitrage bounds
run time	0.201 ± 0.006	0.200 ± 0.006	0.331 ± 0.007

Table 4.3: The run time was measured using 100 evaluations of an American put option with parameters as in 4.2 but with $n_{\text{path}} = 100000$ sample paths. Respecting positivity of the continuation value comes at virtually no computational cost whereas respecting its no-arbitrage bounds increases the run-time by about 50%. All measurements were performed on an Intel Core i7 5600U processor with 8 GB of RAM, running Windows 7 and the Anaconda 2 distribution with 64bit Python 2.7.12.

the put option is deep out-of-the money (the value of the underlying asset today $S^{\text{ini}} = 250$ while the strike $K = 100$), only few Monte Carlo paths sample the area around the strike. In this case, the pure Longstaff-Schwartz continuation value (cyan dashed dotted lines) is outside of the no-arbitrage bounds (4.22) (the blue shaded area) almost everywhere.

Figure 4.4 shows the effect on the continuation value (top panel) and the exercise behaviour (bottom panel). Excluding continuation values $c < 0$ (grey) modifies both continuation value and exercise behaviour for a majority of paths. Respecting the upper (blue) and lower (red) bounds (4.22) has little impact on the price: including the upper bound modifies the continuation value for a majority of paths, yet it does not impact the exercise behaviour – owing to the shape of the payoff (see Figure 4.3) – and hence this bound does not impact the resulting price. Respecting the lower bound (red) changes the exercise behaviour at times close to expiry, but the impact on the price is minimal.

Figure 4.5 shows that the difference in the resulting option price between valuations with continuation values bounded by zero from below (green solid line) and continuation values respecting no-arbitrage bounds is statistically insignificant. These are well within the red shaded area indicating the 3σ confidence interval.

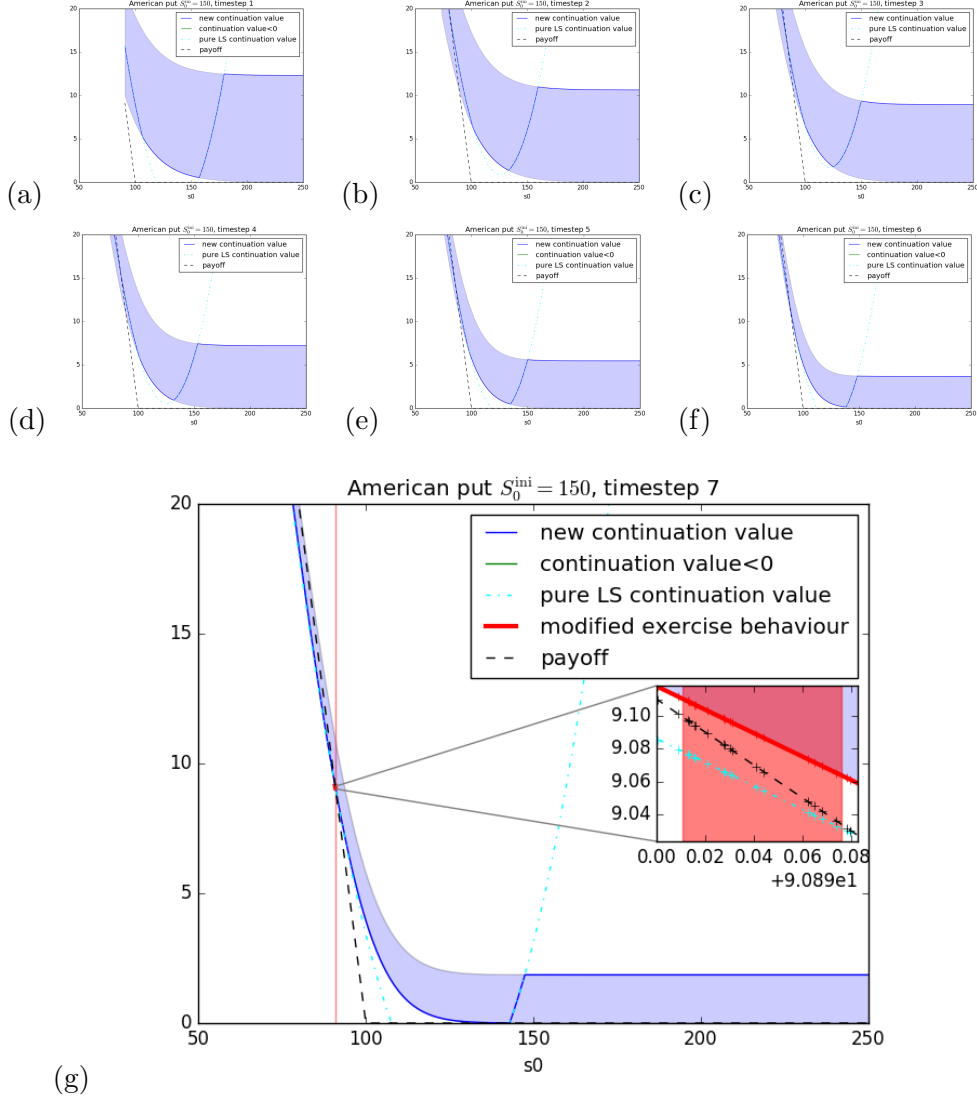


Figure 4.3: Exercise boundary for the American put from Table 4.2 with initial asset price $S_0^{\text{ini}} = 250$ for different time steps. The dashed black line shows the payoff. The solid blue line shows the continuation value respecting the no-arbitrage bounds. The dashed magenta line shows the continuation value ignoring no-arbitrage bounds. The solid green line shows areas where the unmodified continuation value would have been < 0 . The shaded area shows the no-arbitrage bounds. One can see how the continuation is modified due to no-arbitrage bounds almost everywhere. However, the exercise behaviour is only modified in a small segment in time step 7 (panel g): only there, the modified continuation value is above the payoff, while the unmodified continuation value is below the payoff.

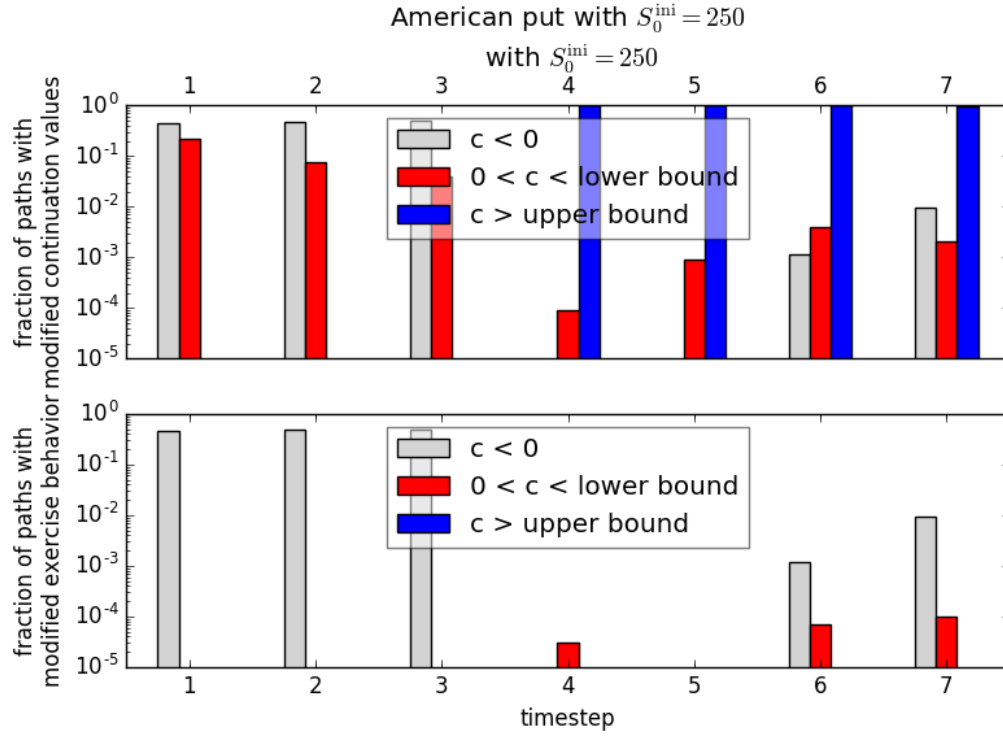


Figure 4.4: Overview over the fraction of paths with modification of the continuation value (top panel) and exercise behaviour (lower panel) for the American put as a function of time t . The light grey bars show the fraction of paths that have continuation values below 0. The red bars show the fraction of paths that have continuation values between 0 and the lower bound. The blue bars show the fraction of paths that have continuation value above the upper bound. Close to expiry, almost all paths have continuation values above the upper bound. Bounding the continuation value by the upper bound has no impact on the exercise behaviour. The influence of the lower bound is limited to a small fraction of paths at times close to expiry.

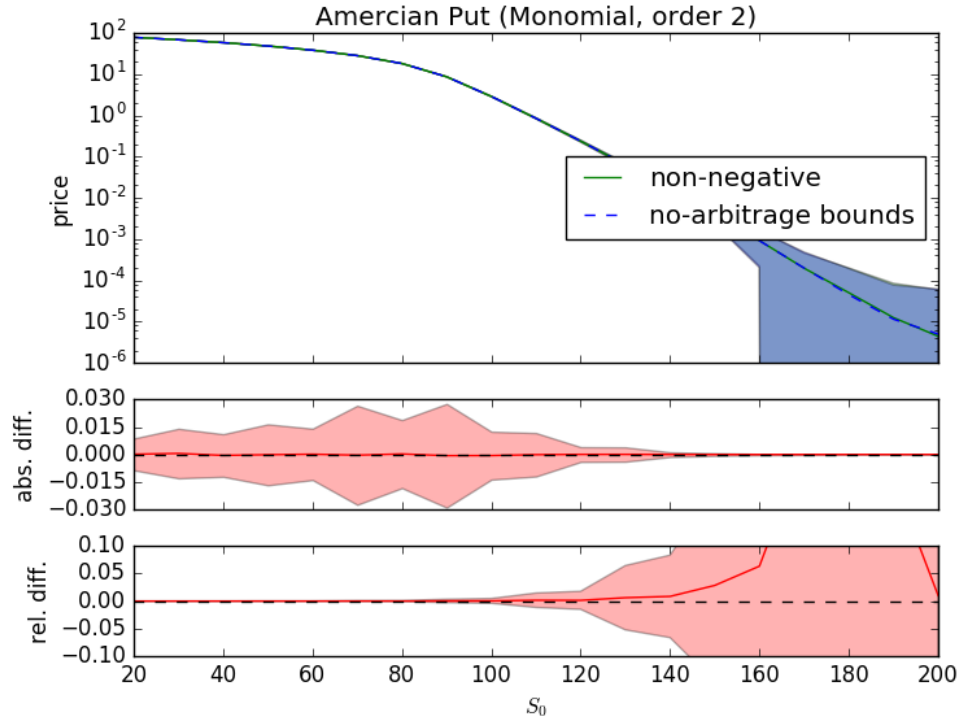


Figure 4.5: The price for an American put on a single asset as a function of initial asset value S_0 with parameters as in Table 4.2. The solid green line uses an Longstaff-Schwartz scheme which bounds the continuation value by 0 from below. The dashed blue line uses an Longstaff-Schwartz scheme which uses the bounds from Equation (4.22) for the continuation value. The red line shows the difference between the two. The indicated error bands cover 3 standard deviation from the n_{rep} valuation runs. Obeying the no-arbitrage bounds for the continuation values has no statistically significant effect on the option price.

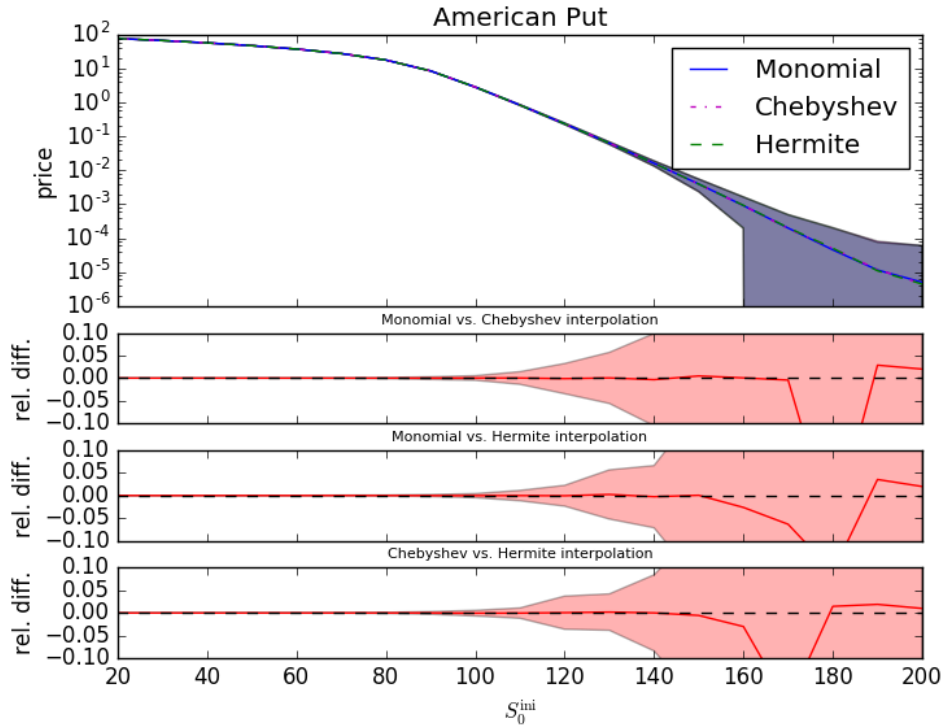


Figure 4.6: Top panel: changing the basis functions from monomials to Chebyshev or Hermite polynomials does not impact the price of the American put. The shaded area shows the 3σ confidence interval. The solid red line in the three bottom panels show the relative differences between the various choices of basis functions for the same set of sampling paths, with the 3σ confidence interval shaded in red. Here, the relative difference is significantly more pronounced – with variation > 1 – but averaging over all sample paths removes this difference.

Effects of changing the function basis

For the American put, there is no noticeable impact on the price when changing the set of basis functions, see Figure 4.6. The top panel shows the price of the put as a function of underlying asset price S_0 , with the shaded area marking the 3σ confidence interval. The bottom panels show the relative difference in price between the three function bases on a path-by-path basis. The same set of random paths $\vec{S}(t)$ was used for all three function bases. The impact the basis choice has on a given path can be quite large – in fact > 1 in relative terms – but averaging over all paths, the effect goes away: there is no significant difference in option price.

Changing the interpolation order from 2 to 3 changes the price of the option for $S_0 \approx 90$, but the effect is still within 3σ of 0 and hence insignificant, see Figure 4.7

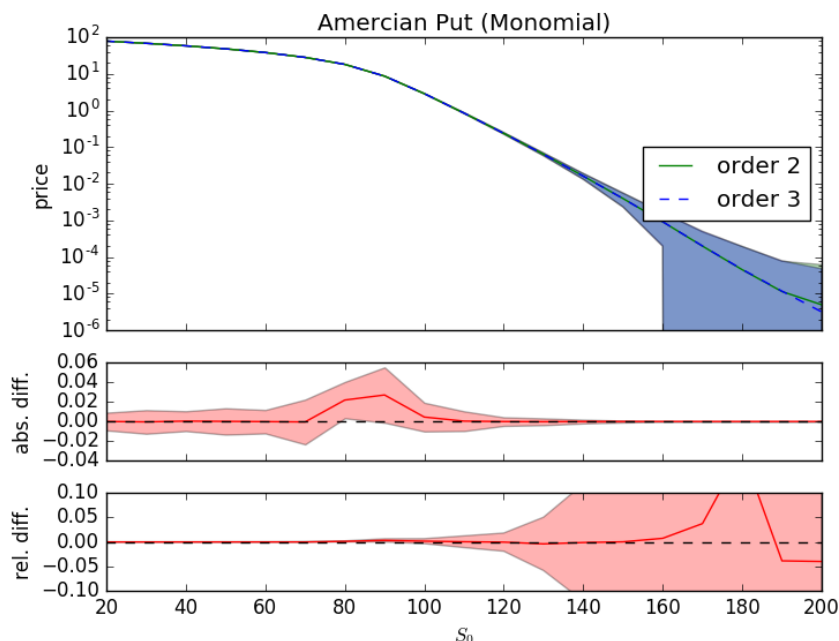


Figure 4.7: Changing the interpolation order for the American put does not impact the price of the option. The bump visible in the absolute difference around $S_0 \approx 90$ is still within 3σ of 0.

4.3 American Max Call

The American max call option for n assets has a payoff of the form

$$h(S, T) = \max \left[\max_i [S_0, S_1, \dots, S_{n-1}] - K, 0 \right], \quad (4.23)$$

where K is the strike. For ease of visualization, we focus on the case of $n = 2$ assets. As noted above, [21] realized that interpolation effects lead to negative continuation values and hence a spurious early exercise region for small values of S_0, S_1 , see Figure 3.4.

Lower and upper bounds

A rather wide upper bound for the continuation value is given by the fact that the price of the max call is bound from above by the sum of the prices of the underlying assets

$$C_a \leq \sum_{i=0}^{n-1} S_i, \quad (4.24)$$

as the claim is easily – but rather poorly – “over-hedged” by buying all underlying assets. However, in case the underlying assets do not pay dividends, we can do better than this.

Instead of outright buying all assets, we could purchase (in this example $n = 2$) American calls on the individual assets. This gives an upper bound of

$$C_a \leq \sum_{i=0}^{n-1} C_a^{\text{ind}}(S_i) = \sum_{i=0}^{n-1} C_e^{\text{ind}}(S_i), \quad (4.25)$$

where $C_{a,e}^{\text{ind}}(S_i)$ is the price of an American (European) call option on individual asset i and in the second equality we assumed that the underlying assets do not pay dividends so that the price of the American call is the same as the European call.

A lower bound on C_a is given by the fact that the American max call is at least as valuable as the most expensive European call on one of its assets

$$C_a = \sup_{\tau} \mathbb{E}_0 \left\{ \max \left[\max_{i \in [0, n-1]} [S_i] - K, 0 \right] \right\} \quad (4.26)$$

$$= \sup_{\tau} \mathbb{E}_0 \left\{ \max_{i \in [0, n-1]} \left[\max[S_i - K, 0] \right] \right\} \quad (4.27)$$

$$\geq \sup_{\tau} \left\{ \max_{i \in [0, n-1]} \left[\mathbb{E}_0 [\max[S_i - K, 0]] \right] \right\}, \quad (4.28)$$

where in the last step we used Jensen's inequality. Hence we find the lower bound

$$C_a \geq \max_{i \in [0, n-1]} \left[C_a^{\text{ind}}(S_i) \right] \geq \max_{i \in [0, n-1]} \left[C_e^{\text{ind}}(S_i) \right], \quad (4.29)$$

which – in contrast to (4.25) is independent of whether the underlying assets pay dividends. All in all, the relevant bound for the continuation value is

$$\boxed{\max_{i \in [0, n-1]} \left[C_e^{\text{ind}}(S_i) \right] \leq C_a \leq \sum_{i=0}^{n-1} C_e^{\text{ind}}(S_i).} \quad (4.30)$$

for underlying assets that do not pay dividends and

$$\boxed{\max_{i \in [0, n-1]} \left[C_e^{\text{ind}}(S_i) \right] \leq C_a \leq \sum_{i=0}^{n-1} S_i,} \quad (4.31)$$

for assets that pay dividends. The price of an American max call on n assets is always larger than the maximum of the price of each European call on the individual assets.

Results of the modifications of Longstaff-Schwartz for non-dividend paying underlying assets

For non-dividend paying underlying assets, the bounds (4.30) have a remarkable consequence. If the underlying assets pay no dividends, the price of a European call is al-

parameter type	parameter	symbol	value
option	initial asset value	$S_0^{\text{ini}}, S_1^{\text{ini}}$	varying
	maturity	T	3
	strike	K	100
	risk-free interest rate	r	0.05
	volatility	σ_0	0.3
		σ_1	0.2
	dividend yield	δ_0	0
		δ_1	0
	correlation	ρ	0
valuation	number of paths	n_{path}	100000
	number of time steps	n_{timestep}	9
	number of repetitions	n_{rep}	100
	Longstaff-Schwartz interpolation order		$1, S_0, S_1, S_0^2, S_0S_1, S_1^2$

Table 4.4: Parameters for the American max call on non-dividend paying underlying assets. Each valuation was performed n_{rep} times.

continuation value	no constraints	non-negative	respecting no-arbitrage bounds
run time	0.50 ± 0.01	0.50 ± 0.01	0.75 ± 0.02

Table 4.5: The run time was measured using 100 evaluations of an American max call without dividends with parameters as in 4.4 but with $n_{\text{path}} = 100000$ sample paths. Again, respecting positivity of the continuation value comes at virtually no computational cost whereas respecting its no-arbitrage bounds increases the run-time by about 50%. All measurements were performed on an Intel Core i7 5600U processor with 8 GB of RAM, running Windows 7 and the Anaconda 2 distribution with 64bit Python 2.7.12.

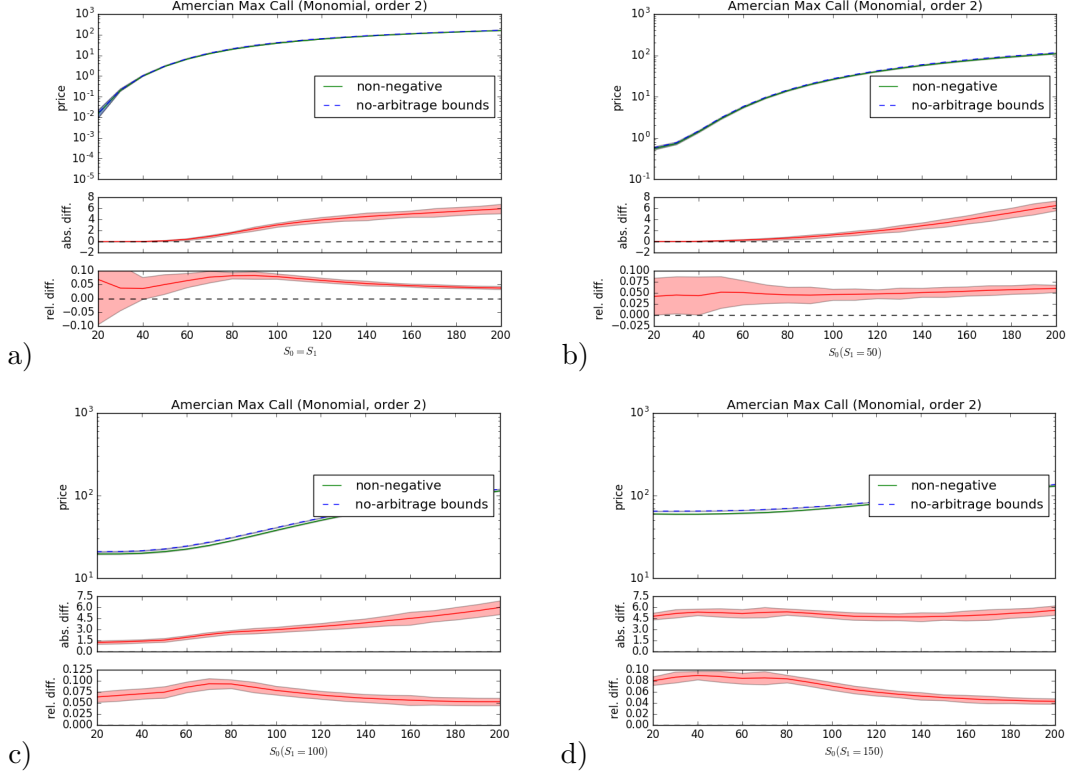


Figure 4.8: The price for an American max call on two non-dividend paying assets as a function of initial asset values a) along the line $S_0^{\text{ini}} = S_1^{\text{ini}}$ b) along the line $S_1^{\text{ini}} = 50$ c) along the line $S_1^{\text{ini}} = 100$ d) along the line $S_1^{\text{ini}} = 150$, with all other parameters as in Table 4.4. The solid green line uses an Longstaff-Schwartz scheme which bounds the continuation value by 0 from below. The dashed blue line uses an Longstaff-Schwartz scheme which uses the bounds from Equation (4.30) for the continuation value. The red line shows the difference between the two. The indicated error bands cover 3 standard deviation from the n_{rep} valuation runs. Enforcing arbitrage-free continuation values (ie preventing early exercise) has a statistically significant impact on the price, changing it by up to 10%.

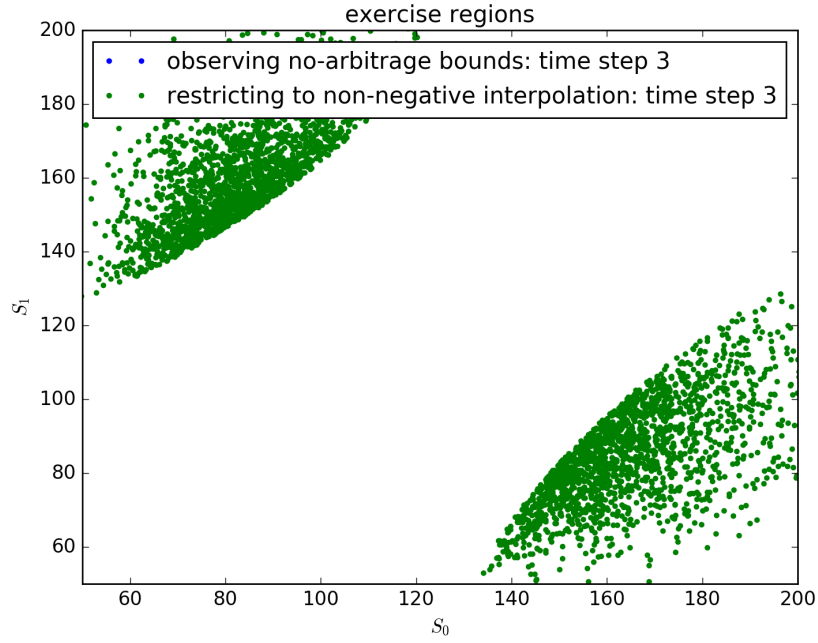
parameter type	parameter	symbol	value
option	initial asset value	$S_0^{\text{ini}}, S_1^{\text{ini}}$	varying
	maturity	T	3
	strike	K	100
	risk-free interest rate	r	0.05
	volatility	σ_0	0.3
		σ_1	0.2
	dividend yield	δ_0	0.1
		δ_1	0.1
	correlation	ρ	0
valuation	number of paths	n_{path}	100000
	number of time steps	n_{timestep}	9
	number of repetitions	n_{rep}	100
	Longstaff-Schwartz interpolation order		$1, S_0, S_1, S_0^2, S_0 S_1, S_1^2$

Table 4.6: Parameters for the American max call on dividend paying underlying assets. Each valuation was performed n_{rep} times, leading to the error bars quoted in Table A.2.

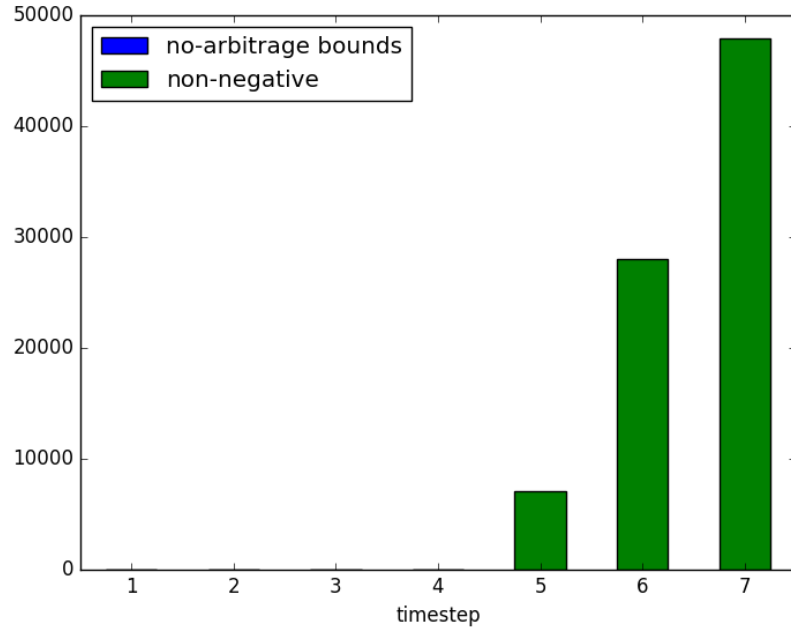
ways larger than its payoff. As consequence, there is no incentive to exercise a corresponding American option early. In particular, this holds for the collection of options $C_e^{\text{ind}}(S_i) = C_a^{\text{ind}}(S_i)$. The lower bound (4.29) implies that the price of a max call is also always larger than its payoff. Hence, a max call on non-dividend paying underlying assets should never be exercised early. This is exactly what we see numerically. Figures 4.10 and 4.11 show that using the bounds (4.30) for the continuation value of an American max call on 2 non-dividend paying assets with parameters in Table 4.4, the continuation value is always above the payoff, so that the option is never exercised early - independent of its moneyness. This has a significant impact ($\approx 10\%$) on the price of the option, see Figure 4.8.

Results of the modifications of Longstaff-Schwartz for dividend paying underlying assets

In case the underlying assets do pay dividends, forcing the continuation value to lie within the no-arbitrage bounds (4.31) impacts the price of the American option only in non-statistically significant way, see Figure 4.12, even though the exercise behaviour changes, see Figure 4.13. At times close to expiry, the presence of the lower bound leads to a modification of the exercise behaviour for about 1% of the sample paths, which does not impact the resulting price.



a)



b)

Figure 4.9: Restricting the continuation value to lie within the bounds of (4.30) prevents early exercise for American max calls on non-dividend paying underlying assets. Panel a) shows the early exercise region at time step 3 for an American max call with parameters as in Table 4.4. The green dots show paths where restricting the continuation value to be non-negative leads to early exercise. Restricting the continuation value by (4.30), there is no early exercise, ie no blue dots. This is in contrast to an American max call on dividend paying assets, see Figure 3.4. Panel b) shows a histogram of early exercise when respecting no-arbitrage bounds (blue) and when restricting the continuation value to be non-negative (green) for initial values $S_0^{\text{ini}} = S_1^{\text{ini}} = 100$. When respecting the no-arbitrage bounds, there is no early exercise, ie no blue bars.

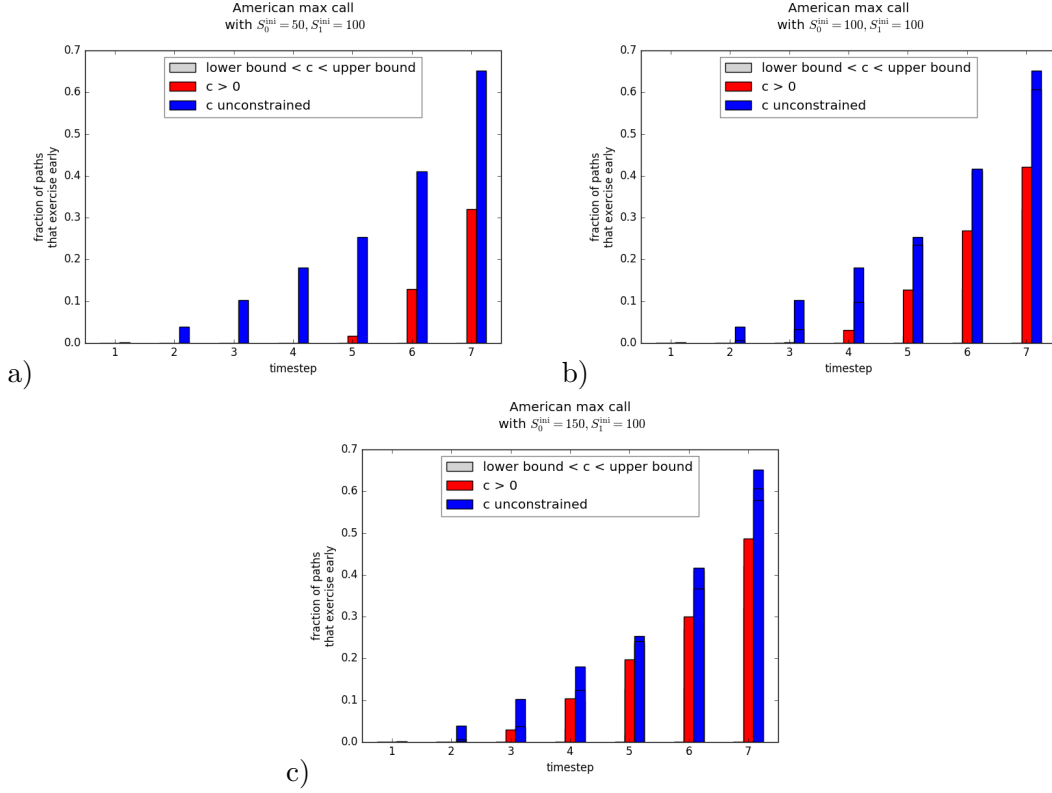


Figure 4.10: Overview over the fraction of paths that exercise early for the American max call on non-dividend paying assets (a) $S_0^{\text{ini}} < S_1^{\text{ini}}$ (b) $S_0^{\text{ini}} = S_1^{\text{ini}}$ (c) $S_0^{\text{ini}} > S_1^{\text{ini}}$ as a function of time t . The absence of light grey bars shows that respecting the no-arbitrage bounds (4.30) prevents early exercise. The red bars show the fraction of paths that exercise early when forcing the continuation value to be positive. The blue bars show the fraction of paths that exercise early when not imposing any constraint on the continuation value.

continuation value	no constraints	non-negative	respecting no-arbitrage bounds
run time	0.50 ± 0.01	0.50 ± 0.01	0.75 ± 0.02

Table 4.7: The run time was measured using 100 evaluations of an American max call with dividends with parameters as in 4.6 but with $n_{\text{path}} = 100000$ sample paths. Again, respecting positivity of the continuation value comes at virtually no computational cost whereas respecting its no-arbitrage bounds increases the run-time by about 50%. All measurements were performed on an Intel Core i7 5600U processor with 8 GB of RAM, running Windows 7 and the Anaconda 2 distribution with 64bit Python 2.7.12.

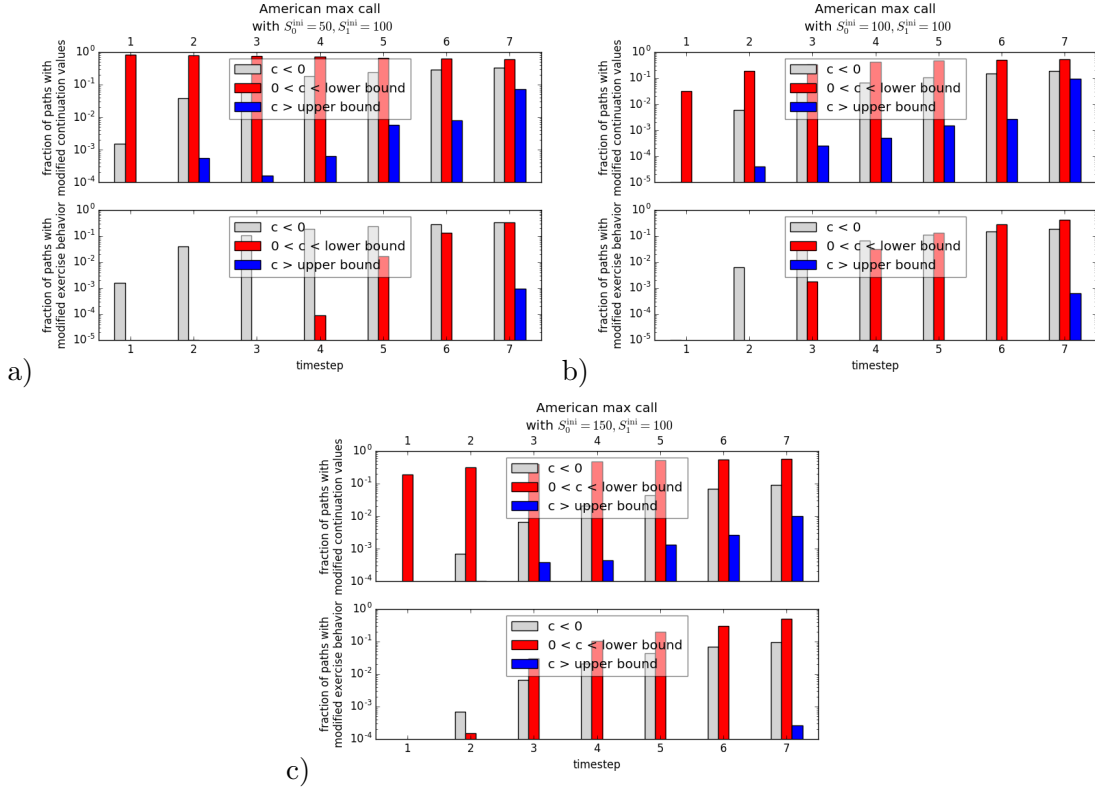


Figure 4.11: Overview over the fraction of paths with modification of the continuation value (top panel) and exercise behaviour (lower panel) for the American max call on non-dividend paying assets (a) $S_0^{\text{ini}} < S_1^{\text{ini}}$ (b) $S_0^{\text{ini}} = S_1^{\text{ini}}$ (c) $S_0^{\text{ini}} > S_1^{\text{ini}}$ as a function of time t . The light grey bars show the fraction of paths that have continuation values below 0. The red bars show the fraction of paths that have continuation values between 0 and the lower bound. The blue bars show the fraction of paths that have continuation value above the upper bound. Close to expiry, almost all paths have continuation values above the upper bound. Bounding the continuation value by the upper bound impacts the exercise behaviour in the pen-ultimate time step. Respecting the lower bound changes the exercise behaviour starting halfway to expiry, with a significant impact on the price, see Figure 4.8.

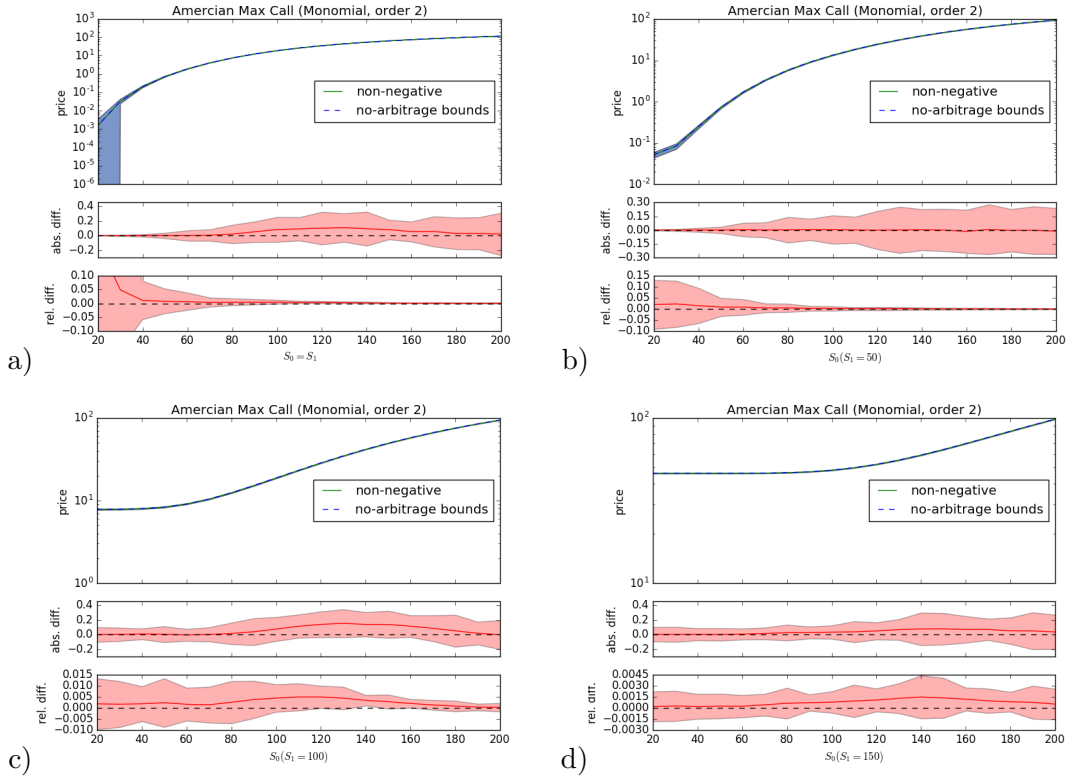


Figure 4.12: The price for an American max call on two dividend paying assets as a function of initial asset values a) along the line $S_0^{\text{ini}} = S_1^{\text{ini}}$ b) along the line $S_1^{\text{ini}} = 50$ c) along the line $S_1^{\text{ini}} = 100$ d) along the line $S_1^{\text{ini}} = 150$, with all other parameters as in Table 4.4. The solid green line uses an Longstaff-Schwartz scheme which bounds the continuation value by 0 from below. The dashed blue line uses an Longstaff-Schwartz scheme which uses the bounds from Equation (4.30) for the continuation value. The red line shows the difference between the two. The indicated error bands cover 3 standard deviation from the n_{rep} valuation runs. There is no statistically significant impact on the price.

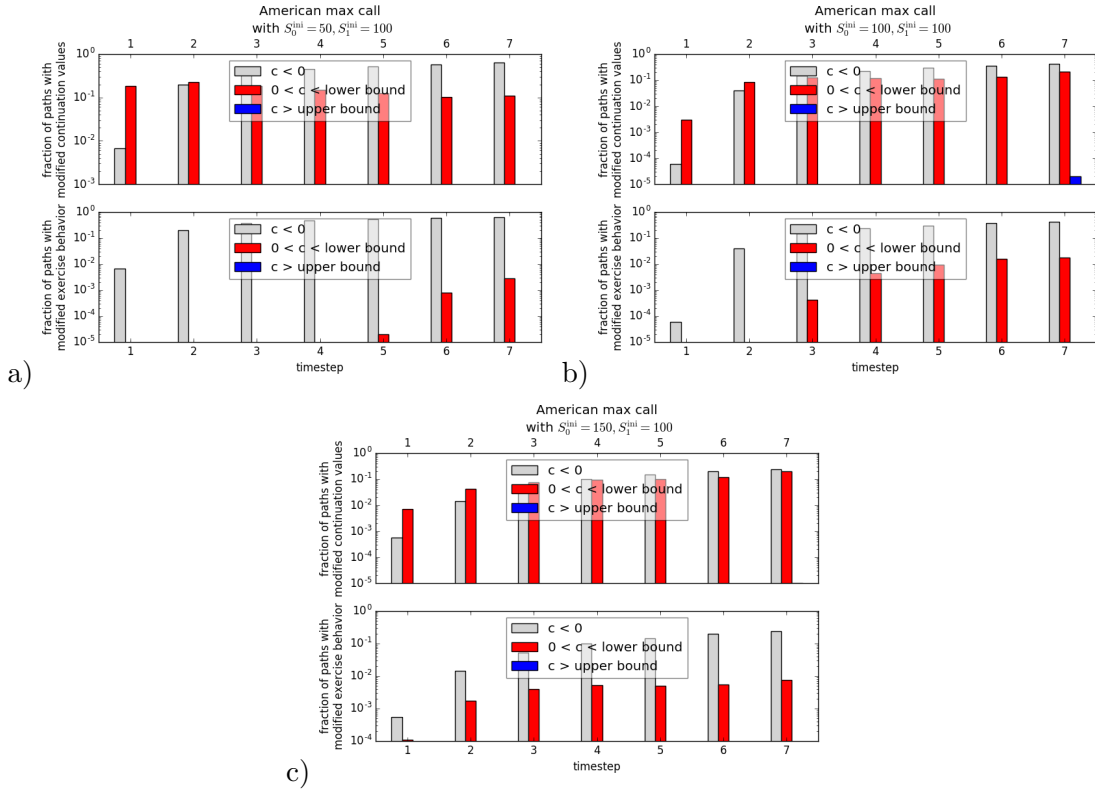


Figure 4.13: Overview over the fraction of paths with modification of the continuation value (top panel) and exercise behaviour (lower panel) for the American exchange option (a) $S_0^{\text{ini}} < S_1^{\text{ini}}$ (b) $S_0^{\text{ini}} = S_1^{\text{ini}}$ (c) $S_0^{\text{ini}} > S_1^{\text{ini}}$ as a function of time t . The light grey bars show the fraction of paths that have continuation values below 0. The red bars show the fraction of paths that have continuation values between 0 and the lower bound. The blue bars show the fraction of paths that have continuation value above the upper bound. Close to expiry, almost all paths have continuation values above the upper bound. Bounding the continuation value by the upper bound has no impact on the exercise behaviour. Respecting the lower bound changes the exercise behaviour mostly closer to expiry independent of the option's moneyness. Despite this, the effect on the option price remains statistically insignificant.

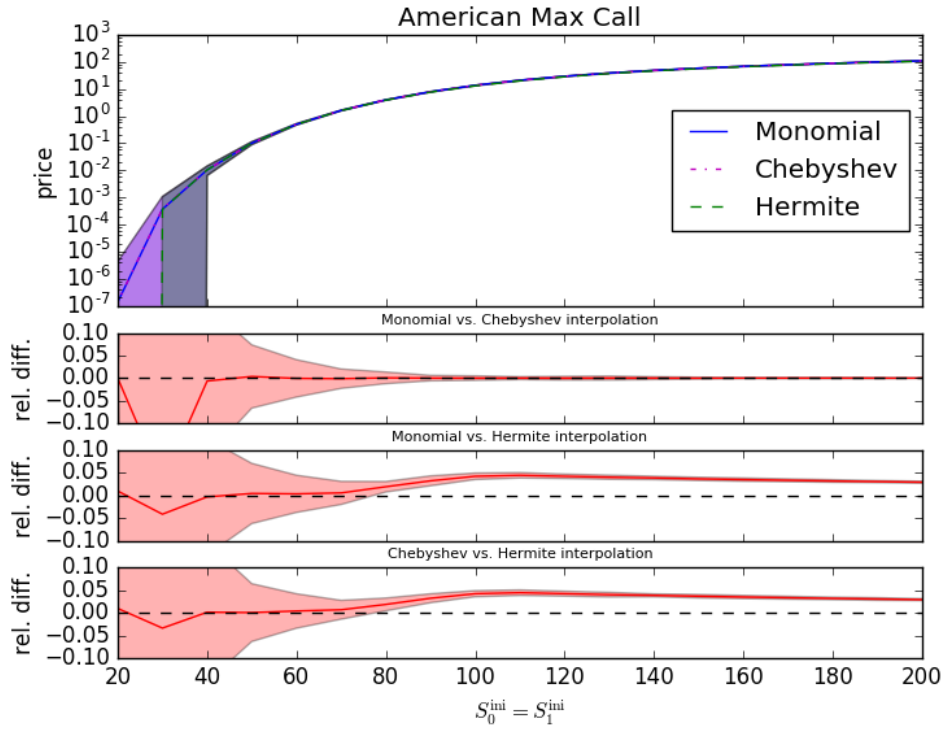


Figure 4.14: Changing the basis function from monomials to Chebyshev polynomials does not impact the price of the American max call. Using Hermite Polynomials changes the price. The shaded area shows the 3σ confidence interval. The solid red line in the three bottom panels show the relative differences between the various choices of basis functions for the same set of sampling paths, with 3σ confidence interval shaded in red.

Effects of changing the function basis

For the American max call on dividend-paying assets, there is a noticeable $\approx 5\%$ impact on the price when changing the set of basis functions to Hermite polynomials, and no impact when using Chebyshev polynomials, see Figure 4.14. The top panel shows the price of the put as a function of underlying asset price $S_0 = S_1$, with the shaded area marking the 3σ confidence interval. The bottom panels show the relative difference in price between the three function bases on a path-by-path basis. The same set of random paths $\vec{S}(t)$ was used for all three function bases.

Changing the interpolation order from 2 to 3 impacts the price statistically significantly by $\approx 0.5\%$, see Figure 4.15.

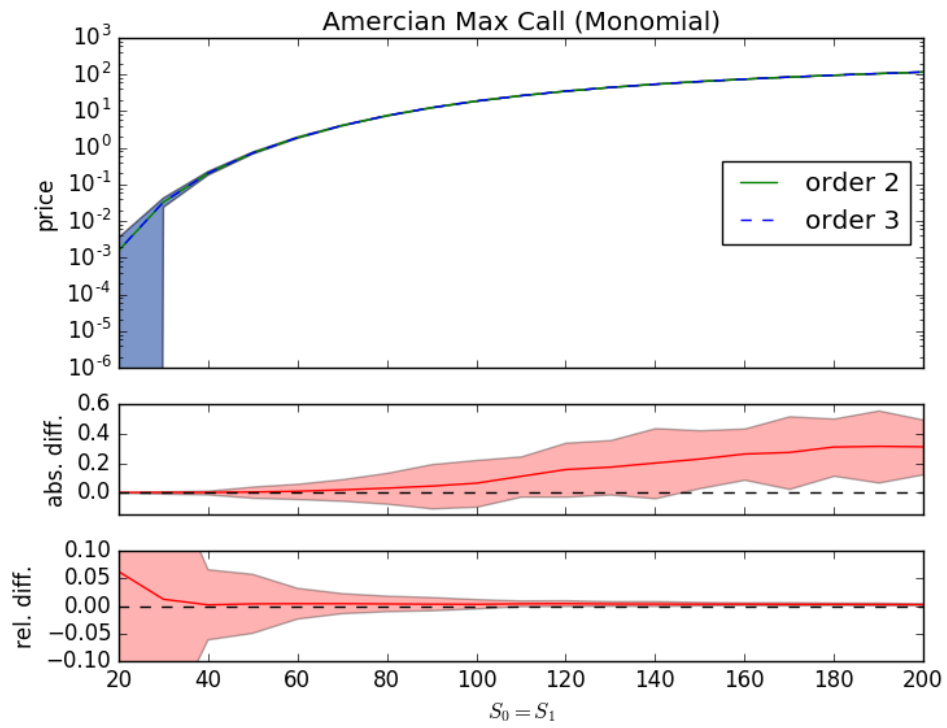


Figure 4.15: Changing the interpolation order for the American max call has a statistically significant impact on the price of the option.

4.4 American Exchange Option

An exchange option for two assets S_0, S_1 gives the option holder the right to exchange asset S_1 for asset S_0 with potential correlation ρ between the assets, each asset with volatility σ_i , and dividend yield y_i , $i = 0 \dots 1$. Hence, the payoff is given by the following expression

$$h(S, T) = \max [S_0 - S_1, 0] . \quad (4.32)$$

Lower and upper bounds

For the European exchange option, [41] showed that the price at time $t < T$ is given by

$$E_e = S_0 e^{-y_0 \tau} \mathcal{N}(d_+) - S_1 e^{-y_1 \tau} \mathcal{N}(d_-) , \quad (4.33)$$

where \mathcal{N} is the cumulative distribution function of the Gaussian random variable, $\tau = T - t$ the time to expiry,

$$d_{\pm} = \frac{\ln \left(\frac{S_0}{S_1} \right) + (y_1 - y_0 \pm \frac{1}{2} \hat{\sigma}^2)}{\sqrt{\hat{\sigma}^2 \tau}} , \quad (4.34)$$

and $\hat{\sigma}^2 = \sigma_0^2 - 2\rho\sigma_0\sigma_1 + \sigma_1^2$. As American options are at least as valuable as European options, this gives a lower bound for the price E_a of an American exchange option.

Instead of purchasing an exchange option, the option holder could also just purchase asset S_0 . Hence the price of S_0 is also an upper bound for the price of the American exchange option.

$$\boxed{E_e \leq E_a \leq S_0} . \quad (4.35)$$

Results of the modifications of Longstaff-Schwartz

Using the bounds (4.35) for the continuation value of an American exchange option with parameters in Table 4.8, we see a statistically significant impact on the price, see Figure 4.17: the exercise behaviour of options is changed in about 10% of the sample paths due to the inclusion of the lower bound (red), with only a weak dependence on the option's moneyness, see Figure 4.16. This is in contrast to the 1% of paths affected by the inclusion of no-arbitrage bounds on the continuation value for the American max call in Figure 4.13 which does not lead to a statistically significant change in option price.

Effects of changing the function basis

For the American exchange option, there is some impact on the price when changing the set of basis functions, see Figure 4.18. The top panel shows the price of the put as a function

parameter type	parameter	symbol	value
option	initial asset value	S_0^{ini}	varying
		S_1^{ini}	100
	maturity	T	3
	strike	K	100
	risk-free interest rate	r	0.05
	volatility	σ_0	0.2
		σ_1	0.4
	dividend yield	δ_0	0.1
		δ_1	0.2
valuation	number of paths	n_{path}	100000
	number of time steps	n_{timestep}	9
	number of repetitions	n_{rep}	100
	Longstaff-Schwartz interpolation order		$1, S_0, S_1, S_0^2, S_0 S_1, S_1^2$

Table 4.8: Parameters of the American exchange option. Each valuation was performed n_{rep} times, leading to the error bars quoted in Table A.3.

continuation value	no constraints	non-negative	respecting no-arbitrage bounds
run time	0.51 ± 0.01	0.50 ± 0.01	0.64 ± 0.01

Table 4.9: The run time was measured using 100 evaluations of an American change option with parameters as in 4.8 but with $n_{\text{path}} = 100000$ sample paths. Again, respecting positivity of the continuation value comes at virtually no computational cost whereas respecting its no-arbitrage bounds increases the run-time by about 50%. All measurements were performed on an Intel Core i7 5600U processor with 8 GB of RAM, running Windows 7 and the Anaconda 2 distribution with 64bit Python 2.7.12.

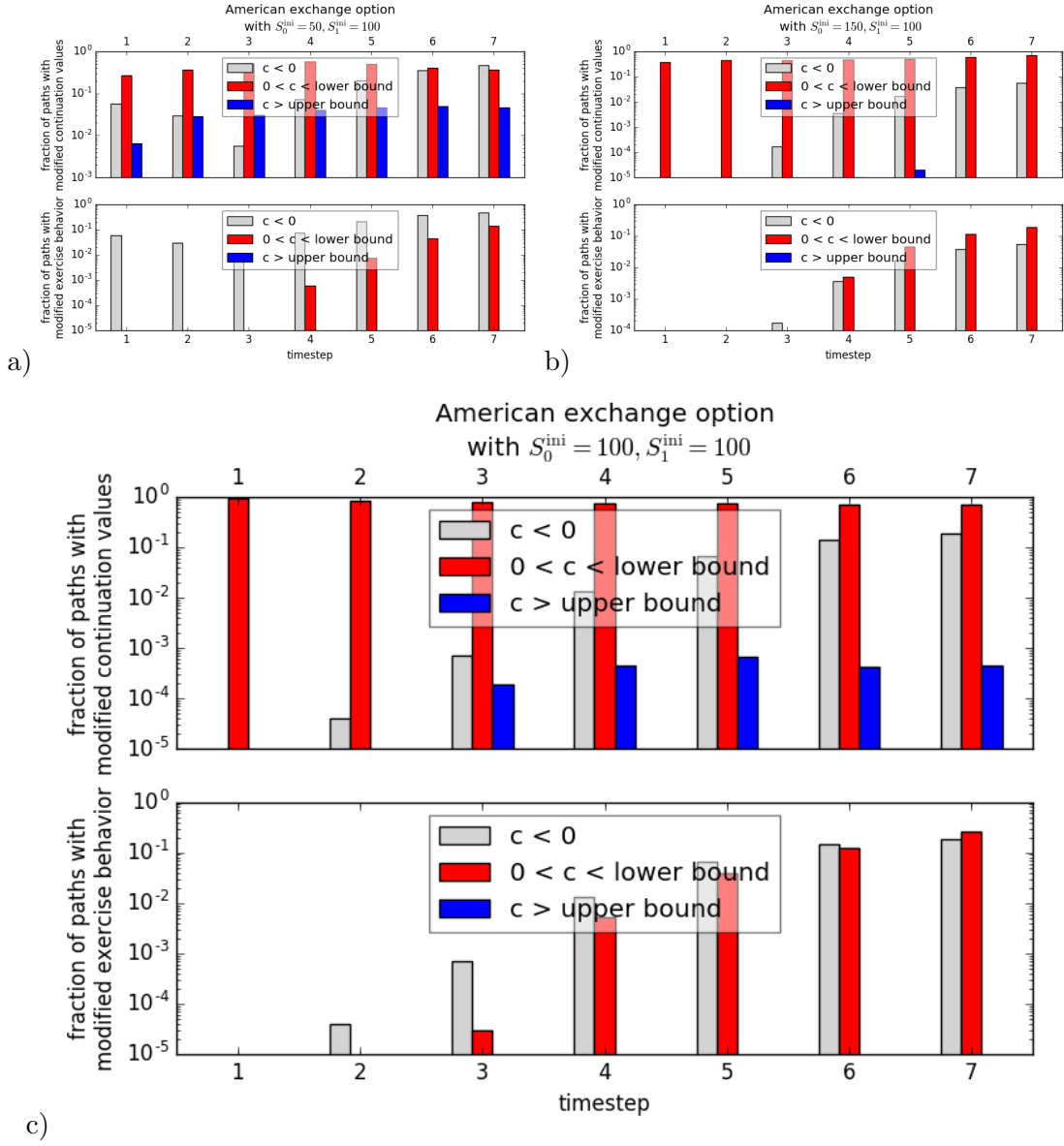


Figure 4.16: Overview over the fraction of paths with modification of the continuation value (top panel) and exercise behaviour (lower panel) for the American exchange option (a) in-the-money (b) out-of-the-money (c) at the money as a function of time t . The light grey bars show the fraction of paths that have continuation values below 0. The red bars show the fraction of paths that have continuation values between 0 and the lower bound. The blue bars show the fraction of paths that have continuation value above the upper bound. Close to expiry, almost all paths have continuation values above the upper bound. Bounding the continuation value by the upper bound has no impact on the exercise behaviour. Respecting the lower bound changes the exercise behaviour mostly closer to expiry independent of the option's moneyness.

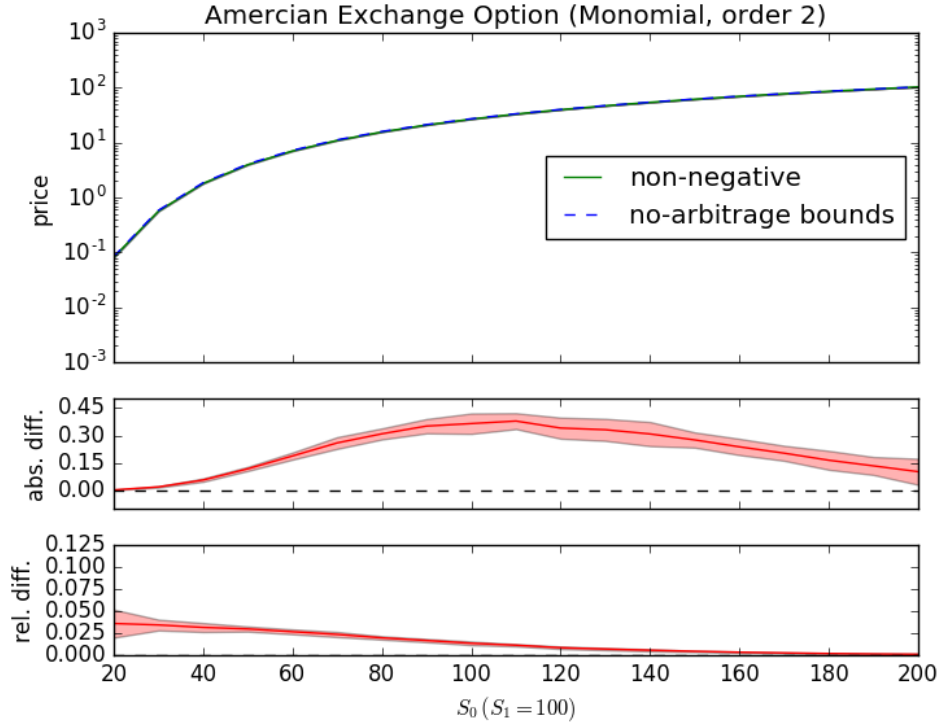


Figure 4.17: The price for an American exchange option as a function of initial asset value S_0^{ini} with parameters as in Table 4.8. The solid green line uses an Longstaff-Schwartz scheme which bounds the continuation value by 0 from below. The dashed blue line uses an Longstaff-Schwartz scheme which uses the bounds from Equation (4.35) for the continuation value. The red line shows the difference between the two. The indicated error bands cover 3 standard deviations from the n_{rep} valuation runs. The smaller the values of S_0^{ini} for fixed S_1^{ini} , the more out-of-the money the option, and the larger the effect of using stronger bounds on the continuation value.

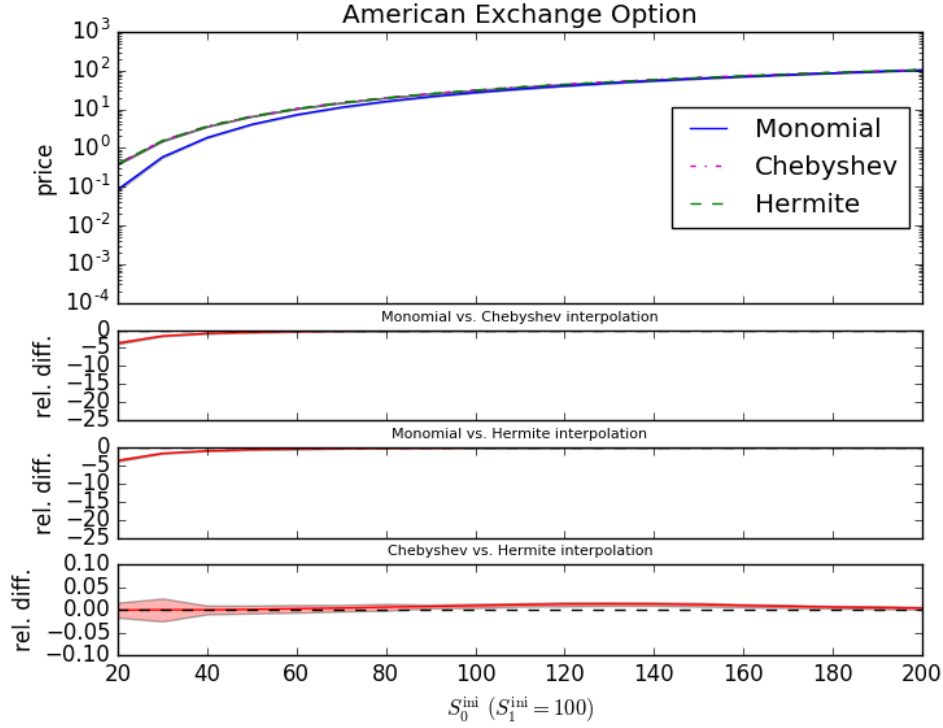


Figure 4.18: Top panel: changing the basis function from monomials to Chebyshev or Hermite polynomials impacts the price of the American exchange option. The shaded area shows the 3σ confidence interval. The solid red line in the three bottom panels show the relative differences between the various choices of basis functions for the same set of sampling paths, with 3σ confidence interval shaded in red. While there is no difference between the Chebyshev and the Hermite basis, there is a large statistically significant difference in the price of the option between using the monomial basis on the one side and the Chebyshev/Hermite basis on the other side.

of underlying asset price S_0^{ini} with fixed $S_1^{\text{ini}} = 100$, and the shaded area marking the 3σ confidence interval. The bottom panels show the relative difference in price between the three function bases on a path-by-path basis. The same set of random paths $\vec{S}(t)$ was used for all three function bases. There is a large statistically significant impact on the price of up $\approx 500\%$ when using Hermite or Chebyshev polynomials as expansion basis for in-the-money options.

Changing the interpolation order from 2 to 3 impacts the price significantly as well when the option is far in-the-money, see Figure 4.19.

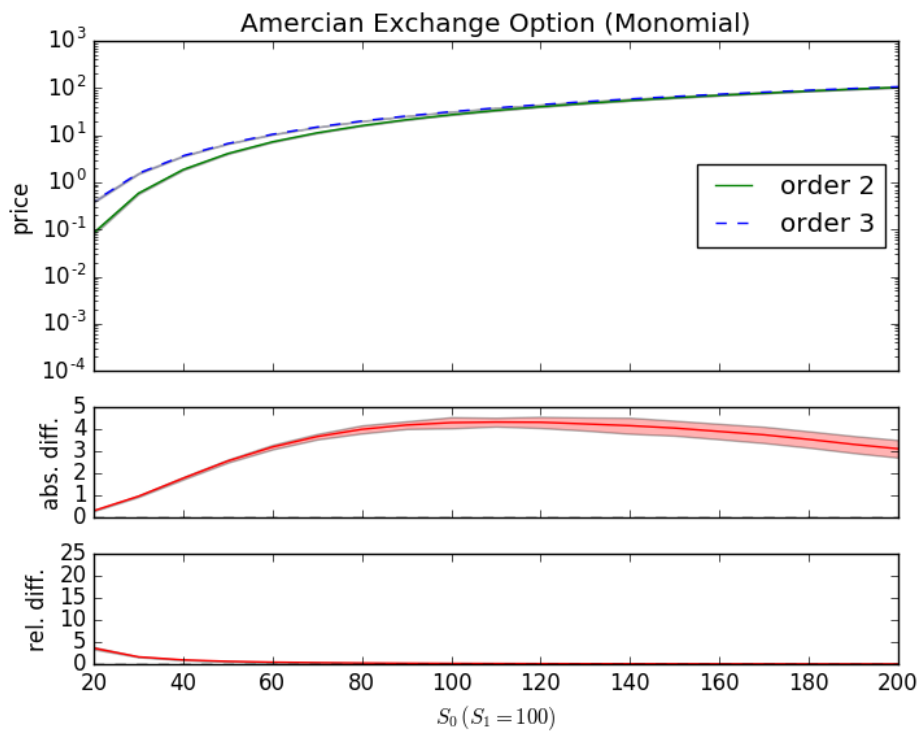


Figure 4.19: Changing the interpolation order for the American exchange option has a systematic impact on the price of the option. The more in-the-money the option gets, the more pronounced the relative difference.

Chapter 5

Conclusions and Outlook

In this thesis, we examined the effects of modifying the Longstaff-Schwartz algorithm, forcing the continuation value to respect no-arbitrage bounds. Implementing constraints for the continuation value to respect no-arbitrage bounds is quite straight-forward. It turns out that the additional computational cost – increasing the run-time by about 50% (see Tables 4.3, 4.7, 4.5, 4.9) – is sometimes worth the increase in accuracy of the price. In general, the better the bound, the more significant the impact on the option price. For the American put, we did not find bounds that were stringent enough to impact its price. On the other hand, the lower bound for the American max call on non-dividend paying assets we found is quite stringent and prevents early exercise with a corresponding a 10% impact on the price. For American max calls on dividend paying assets, the bounds we derived have small but noticeable impact on the price, changing it by about 0.5%. For the American exchange option, we were again able to find bounds that have a noticeable impact on the price of about 3%.

Even if suitable bounds cannot be determined analytically, it might be possible to compute bounds based on numerical schemes - eg by embedding finite difference methods. At first glance it might seem computationally too expensive. But it seems to us that might be not necessary to solve the full future evolution of the price. Just taking a single time step (to the next Monte Carlo step) should suffice.

If one were to find sufficiently stringent upper bounds on prices on the American options, one might even use these directly as continuation values – instead of interpolating the continuation value using regression methods.

While this thesis focuses on enforcing no-arbitrage bounds on the continuation value in the Longstaff-Schwartz approach [1], the same can be done in the context of other regression based methods [24, 25, 26].

References

- [1] Francis A. Longstaff and Eduardo S. Schwartz. Valuing American options by simulation: A simple least-squares approach. *Review of Financial Studies*, pages 113–147, 2001.
- [2] Eduardo S. Schwartz. The valuation of warrants: Implementing a new approach. *Journal of Financial Economics*, 4(1):79–93, January 1977.
- [3] J. Crank and P. Nicolson. A practical method for numerical evaluation of solutions of partial differential equations of the heat-conduction type. *Mathematical Proceedings of the Cambridge Philosophical Society*, 43(1):50–67, 1947.
- [4] Rolf Rannacher. Finite element solution of diffusion problems with irregular data. *Numerische Mathematik*, 43(2):309–327, Jun 1984.
- [5] Michael B. Giles and Rebecca Carter. Convergence analysis of Crank-Nicolson and Rannacher time-marching. *J. Comput. Finance*, 9, 09 2005.
- [6] H. G. Landau. Heat conduction in a melting solid. *Quarterly of Applied Mathematics*, 8(1):81–94, 1950.
- [7] L. Wu and Y.-K. Kwok. A front-fixing finite difference method for the valuation of American options. *The Journal of Financial Engineering*, 6(2):83–97, 1997.
- [8] R.A. Howard. *Dynamic Programming and Markov Processes*. Technology Press of the Massachusetts Institute of Technology, 1960.
- [9] O. Bokanowski, S. Maroso, and H. Zidani. Some convergence results for Howard’s algorithm. *SIAM Journal on Numerical Analysis*, 47(4):3001–3026, 2009.
- [10] M. Hintermüller, K. Ito, and K. Kunisch. The primal-dual active set strategy as a semismooth Newton method. *SIAM Journal on Optimization*, 13(3):865–888, 2002.
- [11] C. Reisinger and J. Witte. On the use of policy iteration as an easy way of pricing American options. *SIAM Journal on Financial Mathematics*, 3(1):459–478, 2012.

- [12] John C. Cox, Stephen A. Ross, and Mark Rubinstein. Option pricing: A simplified approach. *Journal of Financial Economics*, 7(3):229 – 263, 1979.
- [13] R.A. Jarrow and A.T. Rudd. *Option Pricing*. Irwin Series in Marketing. Dow Jones-Irwin, 1983.
- [14] Yisong Tian. A modified lattice approach to option pricing. *Journal of Futures Markets*, 13(5):563–577, 1993.
- [15] Michael J. Brennan and Eduardo S. Schwartz. Finite difference methods and jump processes arising in the pricing of contingent claims: A synthesis. *Journal of Financial and Quantitative Analysis*, 13(3):461–474, 1978.
- [16] Mark Rubinstein. On the relation between binomial and trinomial option pricing models. *The Journal of Derivatives*, 8(2):47–50, 2000.
- [17] Phelim P. Boyle. A lattice framework for option pricing with two state variables. *Journal of Financial and Quantitative Analysis*, 23(01):1–12, March 1988.
- [18] Bardia Kamrad and Peter Ritchken. Multinomial approximating models for options with k state variables. *Manage. Sci.*, 37(12):1640–1652, December 1991.
- [19] Phelim P. Boyle. Options: A Monte Carlo approach. *Journal of Financial Economics*, 4(3):323–338, May 1977.
- [20] J.M. Hammersley and D.C. Handscomb. *Monte Carlo Methods*. Methuen’s monographs on applied probability and statistics. Methuen, 1964.
- [21] Paul Glasserman. *Monte Carlo methods in financial engineering*. Applications of mathematics. Springer, New York, 2004.
- [22] Harald Niederreiter. Quasi-Monte Carlo methods and pseudo-random numbers. *Bull. Amer. Math. Soc.*, 84(6):957–1041, 11 1978.
- [23] H. Niederreiter. *Random Number Generation and Quasi-Monte Carlo Methods*. Society for Industrial and Applied Mathematics, 1992.
- [24] Jacques F. Carrière. Valuation of early-exercise price of options using simulations and nonparametric regression. *Insurance: Mathematics and Economics*, 19:19–30, 12 1996.
- [25] J. N. Tsitsiklis and B. van Roy. Optimal stopping of markov processes: Hilbert space theory, approximation algorithms, and an application to pricing high-dimensional financial derivatives. *IEEE Transactions on Automatic Control*, 44(10):1840–1851, Oct 1999.

- [26] J. N. Tsitsiklis and B. Van Roy. Regression methods for pricing complex American-style options. *IEEE Transactions on Neural Networks*, 12(4):694–703, Jul 2001.
- [27] L. C. G. Rogers. Monte Carlo valuation of American options. *Mathematical Finance*, 12:271–286, 2002.
- [28] Paul Glasserman and Bin Yu. Simulation for American options: Regression now or regression later? In *Working paper DRO-2002-07*. Columbia Business School, 2002.
- [29] P. Wilmott, S. Howison, and J. Dewynne. *The Mathematics of Financial Derivatives: A Student Introduction*. Cambridge University Press, 1995.
- [30] Martin Baxter and Andrew Rennie. *Financial Calculus: An Introduction to Derivative Pricing*. Cambridge University Press, 1996.
- [31] Paul Wilmott. *Paul Wilmott Introduces Quantitative Finance*. Wiley-Interscience, New York, NY, USA, 2nd edition, 2007.
- [32] S. Shreve. *Stochastic Calculus for Finance I: The Binomial Asset Pricing Model*. Springer Finance. Springer New York, 2004.
- [33] S. Shreve. *Stochastic Calculus for Finance II: Continuous-Time Models*. Springer Finance. Springer New York, 2010.
- [34] B. Øksendal. *Stochastic Differential Equations: An Introduction with Applications*. Hochschultext / Universitext. Springer, 2003.
- [35] Martin B. Haugh and Leonid Kogan. Pricing American options: A duality approach. *Oper. Res.*, 52(2):258–270, March 2004.
- [36] G. van Rossum. Python tutorial. Technical Report CS-R9526, Centrum voor Wiskunde en Informatica (CWI), May 1995.
- [37] Stéfan van der Walt, S. Chris Colbert, and Gaël Varoquaux. The numpy array: A structure for efficient numerical computation. *Computing in Science & Engineering*, 13:22–30, 2011.
- [38] Eric Jones, Travis Oliphant, Pearu Peterson, et al. SciPy: Open source scientific tools for Python, 2001–.
- [39] Emmanuelle Clément, Damien Lamberton, and Philip Protter. An analysis of a least squares regression method for American option pricing. *Finance and Stochastics*, 6(4):449–471, Oct 2002.
- [40] William Press. *Numerical recipes: the art of scientific computing*. Cambridge University Press, Cambridge, UK New York, 2007.

- [41] William Margrabe. The value of an option to exchange one asset for another. *Journal of Finance*, 33(1):177–186, March 1978.

Appendix A

Data

S_0	non-negative	non-arbitrage bounds	abs. diff.	rel. diff.
10	88.142157 ± 0.002089	88.142230 ± 0.002005	0.000074 ± 0.001022	0.000004 ± 0.000011
20	78.142377 ± 0.004028	78.142284 ± 0.003863	-0.000093 ± 0.001913	0.000006 ± 0.000024
30	68.142554 ± 0.005688	68.142449 ± 0.005632	-0.000105 ± 0.001692	0.000008 ± 0.000023
40	58.141908 ± 0.007244	58.142437 ± 0.007833	0.000529 ± 0.005466	0.000030 ± 0.000090
50	48.142651 ± 0.009512	48.142167 ± 0.009245	-0.000484 ± 0.004724	0.000028 ± 0.000095
60	38.142485 ± 0.010969	38.143079 ± 0.010604	0.000593 ± 0.003599	0.000021 ± 0.000093
70	28.144002 ± 0.013671	28.144028 ± 0.013598	0.000026 ± 0.005143	0.000051 ± 0.000175
80	18.118473 ± 0.016643	18.119114 ± 0.017375	0.000641 ± 0.009464	0.000151 ± 0.000501
90	8.634453 ± 0.016863	8.635083 ± 0.017598	0.000629 ± 0.006037	0.000180 ± 0.000680
100	2.878659 ± 0.013347	2.878103 ± 0.013676	-0.000556 ± 0.008141	0.000865 ± 0.002693
110	0.848255 ± 0.007397	0.848185 ± 0.007684	-0.000070 ± 0.004344	0.001859 ± 0.004753
120	0.237567 ± 0.003967	0.237866 ± 0.003854	0.000299 ± 0.001875	0.002156 ± 0.007913
130	0.063858 ± 0.001827	0.063797 ± 0.001871	-0.000061 ± 0.001314	0.006690 ± 0.019377
140	0.016204 ± 0.000935	0.016243 ± 0.000943	0.000039 ± 0.000404	0.008293 ± 0.024338
150	0.003941 ± 0.000528	0.003965 ± 0.000516	0.000023 ± 0.000319	0.035430 ± 0.089371
160	0.000920 ± 0.000235	0.000902 ± 0.000223	-0.000018 ± 0.000138	0.072034 ± 0.126726
170	0.000196 ± 0.000093	0.000202 ± 0.000104	0.000006 ± 0.000057	0.169718 ± 0.341403
180	0.000051 ± 0.000050	0.000048 ± 0.000051	-0.000002 ± 0.000021	0.178090 ± 0.344763
190	0.000014 ± 0.000024	0.000015 ± 0.000032	0.000002 ± 0.000022	0.153867 ± 0.770102
200	0.000005 ± 0.000018	0.000004 ± 0.000017	-0.000001 ± 0.000007	0.040000 ± 0.196946

Table A.1: The price for an American put on a single asset as a function of initial asset value S_0 with parameters as in Table 4.2, see also Figure 4.5.

S_0	non-negative	non-arbitrage bounds	abs. diff.	rel. diff.
10	0.000000	0.000000	0.000000	0.000000
20	0.000000 \pm 0.000001	0.000000 \pm 0.000001	0.000000	0.000000
30	0.000388 \pm 0.000230	0.000378 \pm 0.000239	-0.000010 \pm 0.000155	0.459253 \pm 3.000097
40	0.010285 \pm 0.001324	0.010350 \pm 0.001356	0.000065 \pm 0.000549	0.030424 \pm 0.052247
50	0.101693 \pm 0.004264	0.101701 \pm 0.004303	0.000008 \pm 0.001204	0.004314 \pm 0.011074
60	0.500773 \pm 0.009074	0.501446 \pm 0.009637	0.000673 \pm 0.004594	0.002635 \pm 0.008948
70	1.630755 \pm 0.015936	1.629808 \pm 0.015834	-0.000947 \pm 0.007838	0.001553 \pm 0.004564
80	3.998039 \pm 0.026559	3.998416 \pm 0.026612	0.000377 \pm 0.007167	0.000339 \pm 0.001769
90	8.005907 \pm 0.038713	8.004688 \pm 0.038413	-0.001219 \pm 0.009923	0.000225 \pm 0.001222
100	13.791688 \pm 0.049244	13.795077 \pm 0.047628	0.003389 \pm 0.033217	0.000532 \pm 0.002376
110	21.185796 \pm 0.053214	21.202138 \pm 0.055496	0.016342 \pm 0.020963	0.000835 \pm 0.000937
120	29.799022 \pm 0.054810	29.838405 \pm 0.058201	0.039382 \pm 0.022459	0.001322 \pm 0.000754
130	39.167117 \pm 0.058279	39.217710 \pm 0.057729	0.050593 \pm 0.021873	0.001339 \pm 0.000434
140	49.007665 \pm 0.066253	49.052103 \pm 0.065431	0.044438 \pm 0.029740	0.001014 \pm 0.000401
150	59.066868 \pm 0.076980	59.104588 \pm 0.077058	0.037719 \pm 0.049833	0.000816 \pm 0.000672
160	69.256490 \pm 0.071620	69.286888 \pm 0.076573	0.030398 \pm 0.041133	0.000544 \pm 0.000499
170	79.505415 \pm 0.077390	79.524128 \pm 0.079495	0.018713 \pm 0.023658	0.000282 \pm 0.000253
180	89.780663 \pm 0.087961	89.790431 \pm 0.088161	0.009767 \pm 0.029602	0.000155 \pm 0.000310
190	100.084276 \pm 0.084760	100.091206 \pm 0.082132	0.006930 \pm 0.034717	0.000142 \pm 0.000324
200	110.389311 \pm 0.096972	110.385106 \pm 0.096270	-0.004205 \pm 0.040984	0.000124 \pm 0.000351

Table A.2: The price for an American max call on two assets as a function of initial asset value $S_0^{\text{ini}} = S_1^{\text{ini}}$ with parameters as in Table 4.4, see also Figure 4.12.

S_0	non-negative	non-arbitrage bounds	abs. diff.	rel. diff.
10	0.021784 ± 0.000856	0.022545 ± 0.000995	0.000761 ± 0.000720	0.038983 ± 0.029697
20	0.382183 ± 0.005257	0.392450 ± 0.005547	0.010267 ± 0.002710	0.026989 ± 0.006779
30	1.515755 ± 0.013286	1.551900 ± 0.014866	0.036145 ± 0.007060	0.023849 ± 0.004664
40	3.573071 ± 0.024680	3.648694 ± 0.024091	0.075623 ± 0.016686	0.021180 ± 0.004696
50	6.531261 ± 0.030587	6.647302 ± 0.034091	0.116041 ± 0.021972	0.017804 ± 0.003197
60	10.287084 ± 0.048432	10.443332 ± 0.051920	0.156248 ± 0.031872	0.015192 ± 0.003109
70	14.730439 ± 0.053618	14.921905 ± 0.056393	0.191465 ± 0.029124	0.012999 ± 0.001985
80	19.781121 ± 0.067288	19.988021 ± 0.072236	0.206900 ± 0.027948	0.010460 ± 0.001414
90	25.330899 ± 0.069419	25.558118 ± 0.072794	0.227218 ± 0.038682	0.008971 ± 0.001530
100	31.336642 ± 0.096506	31.558420 ± 0.112061	0.221778 ± 0.057774	0.007147 ± 0.001550
110	37.690660 ± 0.096162	37.907418 ± 0.095536	0.216758 ± 0.073246	0.005760 ± 0.001927
120	44.383435 ± 0.109207	44.598202 ± 0.119213	0.214767 ± 0.061756	0.004841 ± 0.001388
130	51.371249 ± 0.097686	51.573965 ± 0.104755	0.202716 ± 0.037972	0.003946 ± 0.000740
140	58.645242 ± 0.120121	58.836541 ± 0.130789	0.191299 ± 0.079665	0.003343 ± 0.001145
150	66.155779 ± 0.112623	66.319693 ± 0.114619	0.163914 ± 0.067903	0.002597 ± 0.000667
160	73.863474 ± 0.142523	74.021828 ± 0.149589	0.158354 ± 0.079819	0.002210 ± 0.000937
170	81.796131 ± 0.136763	81.928089 ± 0.127363	0.131959 ± 0.078388	0.001737 ± 0.000711
180	89.870755 ± 0.136601	89.988196 ± 0.143779	0.117441 ± 0.071094	0.001399 ± 0.000612
190	98.123643 ± 0.139190	98.232757 ± 0.145931	0.109115 ± 0.085700	0.001182 ± 0.000776
200	106.552147 ± 0.139676	106.638113 ± 0.140231	0.085966 ± 0.077805	0.000965 ± 0.000500

Table A.3: The price for an American exchange option that gives the option holder the right to exchange asset S_1 for asset S_0 as a function of initial asset value S_0^{ini} with parameters as in Table 4.8, see also Figure 4.17.